PERISTALTIC FLOW OF A SECOND GRADE DUSTY FLUID IN AN ENDOSCOPE WITH VISCOUS DISSIPATION

By

SAMINA NAZ

NATIONAL UNIVERSITY OF MODERN LANGUAGES

ISLAMABAD

December, 2023

Peristaltic Flow of a Second Grade Dusty Fluid in an Endoscope with Viscous Dissipation

By

SAMINA NAZ

MS Mathematics, National University of Modern Languages, Islamabad, 2023

A THESIS SUBMITTED IN PARTIAL FULFILMENT OF

THE REQUIREMENTS FOR THE DEGREE OF

MASTER OF SCIENCE

In **Mathematics**

To

FACULTY OF ENGINEERING & COMPUTING

NATIONAL UNIVERSITY OF MODERN LANGUAGES ISLAMABAD

THESIS AND DEFENSE APPROVAL FORM

The undersigned certify that they have read the following thesis, examined the defense, are satisfied with overall exam performance, and recommend the thesis to the Faculty of Engineering and Computing for acceptance.

Thesis Title: Peristaltic Flow of a Second Grade Dusty Fluid in an Endoscope with Viscous Dissipation

Submitted By: Samina Naz **Registration #:** 32 MS/MATH/S21

Master of Science in Mathematics
Title of the Degree

Mathematics
Name of Discipline

Dr. Hadia Tariq _____
Name of Research Supervisor Signature of Research Supervisor

Dr. Sadia Riaz _____
Name of HOD(Math) Signature of HOD(Math)

Dr.Noman Malik _____
Name of Dean(FEC) Signature of Dean(FEC)

Dec , 2023

AUTHOR'S DECLARATION

I Samina Naz

Daughter of Pinin Aman

Registration # 32 MS/MATH/S21

Discipline Mathematics

Candidate of **Master of Science in Mathematics** at the National University of Modern Languages do hereby declare that the thesis **Peristaltic Flow of a Second Grade Dusty Fluid in an Endoscope with Viscous Dissipation** submitted by me in partial fulfillment of MS Math degree, is my original work, and has not been submitted or published earlier. I also solemnly declare that it shall not, in future, be submitted by me for obtaining any other degree from this or any other university or institution. I also understand that if evidence of plagiarism is found in my thesis/dissertation at any stage, even after the award of a degree, the work may be cancelled and the degree revoked.

Signature of Candidate

Samina Naz

Name of Candidate

December, 2023

Date

ABSTRACT

Title: Peristaltic Flow of a Second Grade Dusty Fluid in an Endoscope with Viscous Dissipation.

In the present work, we have discussed the behavior of 2^{nd} grade dusty fluid while passing through an endoscope induced by peristaltic movement. Coupled differential equations have been modelled for both fluid and dust particles. Using the regular perturbation technique by taking 'δ' as a perturbation parameter to obtain the analytical solution of the derived equations. Numerical calculations using DSolver in Mathematica software determined the solutions of the problem. The parameters, including Reynolds number, Prandtl number, wave number, etc were identified as important factors in the transport properties. The velocity of dust grains and fluids, as well as stream function, is analyzed graphically. The findings have potential applications in diverse medical fields, such as understanding gastric fluid flow through the small intestine during endoscopy.

TABLE OF CONTENTS

LISTS OF FIGURES

LIST OF SYMBOLS

u, w: Velocity components in the radial and axial directions for the fluid.

u_s, w_s: Velocity components for solid particles.

r, z: Radial and axial coordinates.

a_1, a_2: Radii of the inner and outer wall surfaces of the endoscope.

b: Wave amplitude.

c: Propagating wave speed.

t: Time.

λ: Wavelength.

ρ: Density of the fluid.

μ: Coefficient of viscosity.

α_1, α_2: Material constants for the second-grade fluid.

κ: Thermal conductivity.

β: Dimensionless quantity.

δ: Non-dimensional parameter.

P: Pressure

T: Temperature.

ΔP: Pressure rise.

Gr: Grashof number.

Re: Reynolds number.

Pr: Prandtl number.

K: Coefficient of resistance.

ψ: Stream function for fluid.

φ: Stream function for dust particles.

θ: Temperature field.

ACKNOWLEDGMENT

I am profoundly grateful to Allah for his unwavering guidance and blessings, which provided the foundation for my strength and perseverance throughout this thesis. I extend my deepest appreciation to Dr. Hadia Tariq, whose invaluable guidance and unwavering support have been instrumental in completing this project. Her expertise and insightful feedback have significantly enriched my academic journey, and I am sincerely thankful for her dedicated mentorship, which has contributed immensely to my overall growth as a scholar. Her commitment to excellence and passion for education serve as a constant source of inspiration. Additionally, I express gratitude to all who supported and encouraged me during this academic endeavor. Your belief in my capabilities has been a driving force, and I am truly appreciative of the collaborative spirit that defined this scholarly pursuit.

DEDICATION

This thesis is dedicated to the pillars of my journey – my parents and teachers. Their unwavering encouragement and support have not just propelled me towards my academic goals, but have infused my path with inspiration. To my parents, your unique traits and invaluable contributions have been the driving force behind my pursuit. Your advice and kindness have been more than just support; they've been the steady winds beneath my wings. I am immensely grateful for the role you've played in shaping this incredible journey.

CHAPTER 1

INTRODUCTION

Peristalsis originates from a Greek term that signifies both compressing and relaxing. Peristalsis is the name given to the phenomenon that occurs when muscles contract and release successively in a channel, passage, or tube, leading to a particular process. It occurs naturally in living organisms through the coordinated contraction and relaxation of smooth muscles present in the walls of various organs and structures. Examples include the peristaltic waves occur in the esophagus, propelling swallowed food and liquid towards the stomach. In the stomach, peristaltic contractions mix and break down partially digested food particles. It moves the partially digested food, called chyme, over the small intestine for the absorption of nutrients and also help in flowing of blood through blood vessels. In the urinary system, peristalsis assists in carrying urine from the kidneys to the bladder using the ureters as a pathway. Peristalsis is important for biological processes, but it also has many applications in different fields of biomedical and industrial sciences. . Medical devices and equipment such as blood pumps, heart-lung machines, and peristaltic pumps use peristalsis to move fluids or air through tubes. These devices can be used in surgical procedures, blood transfusions, and other medical applications where precise and controlled movement of fluids or gases is necessary. These studies aim to deepen our understanding of peristaltic phenomena and their implications in diverse fields.

A noteworthy investigation carried out by Elshehawey *et al.* [1] centered on the incompressible peristaltic motion of a viscous fluid within an asymmetrical channel, employing a porous medium in the process.Their research highlighted the significant impact of the phase change between the two channel walls on transport phenomena. By analyzing the dynamics of peristalsis in this particular configuration, the authors shed light on the complex fluid behavior and its influence on the overall transport process.

Elmaboud *et al.* [2], conducted a numerical study focused on examining the use of gold nanoparticles as carriers for drugs for cancer therapy treatment in peristaltic flow of blood

within physiological vessels. The authors explored the impact of these nanoparticles on the transport behavior within the vessels and provided insights into their potential applications in cancer treatment. Yadav *et al*. [3] looked at the impact of electro osmosis processes on peristaltic pumping and the peristaltic movement of Newtonian fluids via the porous media.

Peristaltic flow can help prevent the backflow of fluid in a tube or vessel. The coordinated contractions of the muscles create a unidirectional flow by squeezing the fluid forward and preventing it from flowing backward. This feature is advantageous in situations where maintaining a one-way flow is crucial, such as in pumping systems or preventing contamination in certain processes. It is often considered gentle and non-invasive compared to other pumping mechanisms. The squeezing action exerted by the muscles on the tube or vessel is less likely to damage delicate or sensitive materials being transported. This makes peristaltic flow suitable for applications where maintaining the integrity of the fluid or material is important, such as in the handling of live cells, sensitive chemicals, or fragile samples.

The versatility of peristaltic flow extends beyond medicine and biology, finding numerous applications in engineering and industry. In engineering and industrial fields, peristaltic flow finds several applications due to its unique characteristics and advantages. Peristaltic pumps are commonly used in engineering and industrial applications where precise and controlled fluid delivery is required. They are particularly useful in situations where gentle handling of the fluid is necessary, such as in the pharmaceutical, food processing, and chemical industries. Peristaltic pumps are often used for dosing or metering applications, where accurate and consistent flow rates are essential. It is employed in various industrial processes that require accurate and controlled movement of fluids. This includes applications such as ink and pigment dispensing, paint production, chemical dosing, and wastewater treatment. Peristaltic pumps can handle viscous and abrasive fluids, making them suitable for pumping and transferring challenging materials in industrial settings.

Peristaltic flow is used to deliver ink or glue in a precise and controlled way in the printing and packing industries. Peristaltic pumps are used in printing machines to control the flow of ink and keep them from smudging or getting too full. In the same way, peristaltic pumps are used in packaging to dispense glues or sealants in an exact and controlled way.

While peristaltic transport offers several advantages, it also has some limitations that should be considered. Here are some of the limitations associated with peristaltic transport. It can be affected by variations in the flow rate due to changes in the tube diameter,

compressibility of the fluid, and friction between the fluid and the tube. These factors can cause fluctuations in the flow rate, making it less suitable for applications that require highly consistent and uniform fluid delivery. Peristaltic pumps are typically limited in the maximum pressure they can generate. Higher pressures can lead to excessive deformation or rupture of the tubing, limiting the maximum operating pressure. Therefore, peristaltic transport may not be suitable for applications that require high-pressure fluid delivery. Peristaltic transport can be influenced by the properties of the fluid being transported. Fluid viscosity, temperature, and particulate content can affect the efficiency and reliability of peristaltic flow.

Highly viscous fluids or fluids with high particulate content may cause increased tubing wear or clogging, affecting the performance of peristaltic transport. It's important to consider these limitations when evaluating the suitability of peristaltic transport for a specific application.

1.2 Second Grade Fluid

A fluid is a substance that exhibits the capacity to flow and mold itself to the contours of the container it occupies. This state of matter is defined by its capability to undergo deformation in response to applied shear stress or external forces, encompassing both liquids and gases. Liquids, like water, oil, and alcohol, have a relatively high density and aren't easy to squeeze. They have a set amount of space, but they can change shape to fit their container.

Most people think that liquids can't be compressed, which means that when pressure is put on them, their volume stays pretty much the same. Gases like air, nitrogen, and carbon dioxide are less dense than liquids and can be compressed very easily. Gases don't have a set form or volume, and they will fill up the whole space they are in. Changes in pressure and weather can make them shrink or grow. Both liquids and gases exhibit properties of fluids, such as the ability to flow, exert pressure, and transmit forces. Fluid mechanics is the area of physics that explores the behavior and properties of fluids, encompassing fluid flow, buoyancy, and viscosity.

Fluids can be categorized into different types based on their physical properties and behavior. Here are some common types of fluids such as Newtonian Fluids, Non-Newtonian Fluids, Compressible fluids, incompressible fluids and ideal fluids. Newtonian fluids are fluids that obey Newton's viscosity law, which states that shear stress is

proportionally related to the shear strain rate. Newtonian fluids include water, petrol, and most other familiar liquids.

While, Non-Newtonian Fluids: These fluids deviate from Newton's law of viscosity and display complex flow patterns. Fluids that aren't Newtonian can be divided into a few more groups. Shear-thinning or pseudo plastic fluids: The viscosity of these fluids drops as the rate of shear increases. Ketchup, paint, and some kinds of polymer liquids are all good examples. Shear-thickening or dilatant fluids: The viscosity of these fluids gets thicker as the shear rate goes up. A common example is oobleck, which is a mixture of corn flour and water. These fluids require a specific minimum shear stress (yield stress) to begin to flow. Toothpaste as well as certain drilling fluids demonstrate Bingham plasticity. Thixotropic Fluids: When subjected to continuous shear stress, these fluids become less viscous over time. Certain gels and pigments exhibit thixotropic properties.

A second grade fluid is a specific type of non-Newtonian fluid where the relationship between the stress and the strain rate tensor includes up to two derivatives of velocity. While, in a Newtonian fluid, the stress-strain relationship only involves the first derivative of velocity (strain rate), and the viscosity is constant. This simplicity makes Newtonian fluids easier to model and analyze compared to non-Newtonian fluids. This means that the velocity field in a second grade fluid can have up to two spatial derivatives in the stress-strain tensor relationship. The constitutive equation that describes the behavior of a second grade fluid is given by:

$$\tau = \mu \left(\frac{du}{dy}\right) + \lambda \left(\frac{\partial^2 u}{\partial y^2}\right),$$

where ;

τ is the shear stress is the dynamic viscosity,

$\frac{du}{dy}$ is the velocity gradient (rate of strain),

λ is a coefficient that describes the connection between viscosity and how quickly deformation or strain occurs.

The term $\frac{\partial^2 u}{\partial y^2}$ corresponds to the second-order velocity derivative concerning position.

In a second grade fluid, the additional term involving the second derivative of velocity $\frac{\partial^2 u}{\partial y^2}$ accounts for the rate-dependent viscosity. This term allows the viscosity to vary with changes in the rate of strain, making second grade fluids distinct from both Newtonian and other non-Newtonian fluids.

A common example of second grade fluid is toothpaste. When shear stress is applied, it moves easily out of the tube, but when it is at rest, it becomes more viscous and keeps its shape. Ketchup is another familiar example of a second-grade fluid. It requires some force to get it flowing out of the bottle, and then it becomes less viscous and flows more easily. Silly Putty is a flexible, moldable toy with non-Newtonian properties. It behaves like a solid under moderate stress but flows like a liquid when subjected to greater stress or force. Shampoo is frequently a non-Newtonian liquid. Because of the applied stress, it pours readily from the bottle but becomes more viscous and adheres to your hair while at rest.

Second-grade fluids or non-Newtonian fluids have various applications across different fields. Here are some common areas where these fluids find practical use. Fluids that are not Newtonian are used in many industrial processes, like mixing, pumping, and moving materials. Their different viscosities can help control flow rates, reduce turbulence, and improve the general efficiency of a process. Non-Newtonian fluids find widespread application in various personal care products, including lotions, creams, and hair care items. These fluids have appropriate flow, stability, and usage properties, which make the products work better and improve the user experience.

In the field of biology, second-grade fluids (non-Newtonian fluids) have several applications. Blood is a non-Newtonian fluid due to its complex composition and changing shear rates in blood vessels. Understanding blood's non-Newtonian behavior is essential for simulating blood flow patterns, analyzing cardiovascular disorders, and constructing medical devices like artificial heart valves. Second-grade fluids explore cell and tissue mechanics. Researchers can learn about cell mechanics, migration, and tissue engineering by studying cell deformation and flow in response to applied forces.

Non-Newtonian fluids are employed in drug delivery systems. For example, hydrogels and polymer-based carriers with non-Newtonian behavior can provide controlled drug release profiles, protect sensitive drugs, and improve their bioavailability. Mucus secretions in various parts of the body, such as the respiratory and digestive systems, are second-grade fluids. Mucus acts as a protective barrier, and its viscosity changes with shear stress to facilitate clearance of pathogens, particles, and debris. These examples show how biological second-grade fluids have unique rheological properties that are critical for biological processes, tissue function, and cellular dynamics.

The objectives related to second-grade fluids (non-Newtonian fluids) can vary depending on the specific context and application. However, some common objectives associated with the study and understanding of second-grade fluids are following. Firstly, understanding the rheological behavior of these fluids is a primary objective. This involves characterizing their viscosity, shear stress, shear rate, and deformation response to establish the non-Newtonian properties they exhibit. By comprehending the complex behavior of second-grade fluids, researchers and engineers can develop accurate mathematical models and computational tools to predict flow patterns and phenomena.

Rundora and Makinde [4] investigated the magnetohydrodynamic (MHD) flow of a non-Newtonian fluid in a channel containing a saturated porous medium. They accounted for asymmetric Navier slip conditions and convective heating in their investigation. Hina and Yasin [5] investigated the impact of slip effects on the peristaltic flow of a magnetohydrodynamic 2^{nd} grade fluid over an elastic canal with heat and mass transfer.

Another objective is to apply this knowledge in engineering applications. By optimizing systems involving non-Newtonian fluids, such as pumping, mixing, and transportation processes, it becomes possible to control and manipulate viscosity, flow rate, and stability. This objective is important for improving process efficiency, reducing energy consumption, and ensuring desired product outcomes. Overall, the objectives of second-grade fluids encompass understanding their rheological behavior, predicting and modeling fluid flow, optimizing processes, formulating materials, and applying their unique properties in various fields of study and application. By achieving these objectives, advancements can be made in engineering, materials science, biology, and healthcare, leading to improved technologies and enhanced understanding of complex fluid dynamics.

1.3 Dusty Fluid

The word "dusty fluid" usually refers to a mixture or suspension of solid particles (dust) in a fluid medium. It is characterized by the presence of fine particulate matter, such as dust, powder, or granular materials, dispersed and suspended in a liquid or gas.

Solid particles in a dusty fluid are often much larger than the fluid's molecules or atoms, and they interact with the surrounding medium via numerous phenomena such as gravity, Brownian motion, and fluid drag. The particles can behave differently based on their size, concentration, and fluid characteristics, resulting in interesting and complex phenomena.

Dusty fluids can be found in a variety of natural and industrial environments. Dusty fluids in nature include volcanic ash suspended in the air, sediment-laden rivers, and atmospheric pollution. Dusty fluids can be found in industrial processes such as powder handling, aerosol sprays, and combustion systems.

Dusty fluids can be found in various contexts, ranging from natural resources to biological fluids and laboratory applications. Crude oil, extracted from underground reservoirs, serves as a prime example. It consists of a mixture of hydrocarbons and often contains suspended solid particles known as sediments. These particles form a dusty fluid within the oil, affecting its flow properties, potentially leading to clogging or erosion in pipelines, and influencing the refining process. Similarly, unrefined petroleum, which also undergoes extraction processes but hasn't undergone extensive refining, may contain solid impurities or sediments, such as sand, clay, or rust. These impurities create a dusty fluid within the petroleum, necessitating additional processing steps to remove them during refining.

Human urine with stones is a biological example of a dusty fluid. When individuals have urinary stones, the movement of these stones through the urinary system can introduce solid particles into the urine, such as calcium oxalate or uric acid crystals. This results in a dusty fluid within the urine, which may cause discomfort and indicate underlying medical concerns that require care. When platelets, fibrin, and other blood components gather and solidify, blood clots form. The clot of blood that forms is a dusty fluid with solid particles suspended in liquid plasma. Blood clots are important in wound healing and preventing excessive bleeding, but if they grow improperly or become dislodged, they can cause blockages in blood vessels.

Laboratory applications often involve the creation of suspensions, such as a glucose particle suspension. In this case, solid glucose particles are dispersed or suspended in a liquid medium, like water or a sugar solution. The suspended glucose particles form a dusty fluid within the liquid. These suspensions can be utilized in laboratory experiments, pharmaceutical formulations, or food applications where a homogeneous mixture or controlled release of glucose particles is desired.

In their research, Prasannakumara *et al.* [6] explored the melting behavior within a dusty fluid subjected to magnetohydrodynamic (MHD) stagnation point flow. This investigation was conducted on a stretching sheet and considered the impacts of thermal radiation as

well as the presence of a non-uniform heat source or sink. The authors examined the flow characteristics and analyzed the effects of these factors on the melting process.

Turkyilmazoglu [7] presented a model for the movement and heat of a two-phase granular fluid under magnetohydrodynamic conditions over deforming isothermal surfaces. The research by Siddiqa *et al.* [8] explored the radiative heat transfer analysis of non-Newtonian dusty Casson fluid flow along a complex wavy surface. The study's findings revealed a substantial increase in the rate of heat transfer with the penetration of the radiation parameter and mass concentration parameter into the system.

1.4 Heat Transfer

Heat transfer occurs when thermal energy is exchanged between two or more objects or systems due to a difference in temperature. It manifests itself in several ways, including conduction, convection, and radiation.

Conduction is the transport of heat via direct contact between objects or within a substance. It occurs when hotter molecules transfer thermal energy to nearby colder molecules, causing them to vibrate and increase in temperature. Metals are generally good conductors of heat due to the free mobility of electrons within their atomic structure. Some examples demonstrate how conduction allows heat to transfer through direct contact between objects or within materials are following. When we contact a hot pan, heat is transferred from the pan to our hand. The metal of the pan transfers thermal energy to our skin through direct contact, causing us to feel hot. Another common examples are heating a pot of water, walking barefoot on hot sand, ironing clothes, heating a metal spoon in hot soup and cooling with an ice pack.

Fluids, encompassing both liquids and gases, facilitate the transfer of heat through convection. As a fluid is heated, its density decreases, causing it to ascend and generate a flowing pattern known as a convection current. As the heated fluid moves, it carries thermal energy away from the heat source. Conversely, cooler fluid descends, creating a cycle of heat transfer. This process is commonly observed in natural phenomena like boiling water or atmospheric circulation.

Radiation denotes the propagation of heat via electromagnetic waves, with infrared radiation being a prominent example. Notably, radiation differs from conduction and convection in that it can manifest itself in environments without matter, such as a vacuum,

or without objects physically touching each other. Any object with a temperature above absolute zero emits thermal radiation. This type of heat transfer is responsible for the warming effects of sunlight and the emission of heat from objects like electric heaters or fires.

The impact of heat transmission on the peristaltic flow of a 2^{nd} grade dusty fluid in a duct can have several significant consequences. Heat transfer can cause temperature variations within the fluid, leading to changes in its viscosity and the behavior of the suspended solid particles. These variations in viscosity and particle suspension can alter the flow resistance, flow patterns, and particle transport characteristics during peristaltic motion. Additionally, heat-induced thermal expansion or contraction of the tube and the fluid can influence the tube's geometry and compliance, affecting the propagation of the peristaltic wave and the overall flow behavior. The interplay between the particles and the fluid can also be influenced by heat transfer, leading to changes in particle-fluid interaction forces, particle dynamics, and flow resistance. Furthermore, heat transfer can induce thermal convection within the fluid, affecting the particle distribution, mixing, and flow patterns during peristaltic flow.

Heat transfer has a significant impact on the flow of peristaltic fluid through small tubes, and this impact is crucial in various medical applications. For instance, during an endoscopy, when gastric fluid passes through the small intestine, understanding heat transfer is essential to comprehend the peristaltic mechanism. Heat transfer also plays a vital role in fields like geophysics and engineering, encompassing tasks such as geothermal energy transport, thermal insulation, handling porous materials, drying processes, and enhancing fossil fuel and oil recovery. In medicine, analyzing heat transfer is an effective method to calculate blood flow rates, considering factors like heat dissipation and initial temperature conditions. This information provides insights into tissue characteristics. A dilution technique, involving localized heat injection or generation, can be employed to evaluate flow patterns and measure heat clearance. This simplified approach to heat transfer analysis facilitates data collection and enhances our understanding of biological and physical processes. By studying peristalsis with heat transfer, researchers can explore methods to optimize heat transfer processes and improve overall system efficiency. This is applicable in various fields, including energy systems, industrial processes, and thermal management in medical devices.

1.5 Endoscope

An endoscope is a slender, tube-like optical instrument that is used in medical investigations to examine internal parts of the body. It consists of a flexible or rigid tube with a light source and a camera or lens at one end. The other end of the endoscope is connected to various instruments that can be used for procedures like biopsies or surgeries.

The application of an endoscope in the peristaltic movement of dusty fluid involves utilizing the endoscope's capabilities to visualize and investigate the flow of fluids containing particles or dust in various medical and industrial settings. The peristaltic movement of an endoscope plays a vital role in medical investigations. Peristalsis refers to the coordinated muscle contractions and relaxations that generate wave-like motions. This rhythmic movement is similar to how our digestive system propels food through the intestines. In the context of an endoscope, peristalsis enables the flexible tube to navigate through the body's internal passages in a smooth and controlled manner, following the natural curves and contours of the organs being examined. This peristaltic movement is crucial for effectively navigating the endoscope through narrow and winding pathways, such as the gastrointestinal tract or the respiratory system. It enables medical professionals to reach the desired target area for examination or intervention, minimizing discomfort and potential damage to surrounding tissues.

In industrial applications, the endoscope can be customized with tools or sensors suited for specific inspection or fluid manipulation tasks.

Despite the significant advantages offered by endoscopes, there are limitations to consider when studying the peristaltic flow of a second-grade dusty fluid. The complex rheological behavior of non-Newtonian fluids, combined with the presence of suspended particles, introduces challenges in accurately predicting flow patterns and interactions. The influence of factors such as particle size, concentration, and distribution on the peristaltic flow behavior within the endoscope may not be fully understood or easily quantified. Furthermore, variations in fluid viscosity and rheology due to shear thinning properties of second-grade fluids can further complicate the flow dynamics.

Furthermore, the peristaltic motion of an endoscope is equally important in clinical investigations. It enables healthcare professionals to safely explore internal organs for

diagnostic and therapeutic purposes. During procedures like biopsies or therapeutic interventions, the peristaltic movement guides the instruments to the precise location, reducing the risk of damage to surrounding tissues and improving the accuracy of the procedure.

Thesis Contribution

In our thesis, we studied the behavior of a second grade dusty fluid model while flowing through an endoscope. We specifically tried to understand viscous dissipation in this context.

Thesis Organization

In our thesis, chapter 1 is about the introduction of thesis title. Chapter 2 provides a literature review related to our topic, delving into existing research and knowledge. In Chapter 3, we present basic definitions used in our thesis, ensuring clarity and understanding of key terms. Chapter 4 reviews the work conducted by Tariq and Khan, building on their contributions to our field of study. Chapter 5 extends the discussion from Chapter 4, adding depth to the exploration of our research topic. Lastly, Chapter 6 concludes the findings from Chapter 5, bringing the research to a comprehensive and insightful close.

CHAPTER 2

LITERATURE REVIEW

Over the past few years, there has been a growing fascination among researchers with investigating peristalsis and its various manifestations in different scenarios. Peristalsis has been the subject of extensive analytical, numerical, and experimental investigations. Under the suppositions of a long wavelength and a low Reynolds number, Tripathi [9] conducted a study on the peristaltic transport of a viscoelastic fluid within a cylindrical tube using a fractional second-grade model. The author obtained an analytical solution to the problem using Caputo's definition. A numerical analysis was performed to explore how the friction force and pressure through one wavelength are influenced by the fractional parameter, material constant, and amplitude. From the findings, it becomes evident that pressure exhibits an inverse relationship with the fractional parameter, while it displays a direct relationship with the material constant or time magnitude. In their research, Vaidya *et al.* [10] investigated how slip influences the peristaltic flow of a non-Newtonian Jeffrey fluid through a tube that is inclined. Moreover, their research revealed practical applications in exploring how chyme functions as it progresses through the gastrointestinal tract, shedding light on its illuminating properties.

Several recent research works have explored the applications of peristalsis, including [11], [12], [13], [14], [15], and [16]. Esser *et al*. [17] discussed the peristaltic pumping principle in a comparative topical overview, examining its applications in living nature, engineering, and bio mimetics. Asha and Sunitha [18] investigated the influence of heat radiation and Hall impacts on peristaltic blood flow with doubled diffusion in an asymmetric channel in the presence of nanoparticles. This study was carried out by assuming long wavelengths and low Reynolds numbers to explore how the friction force and pressure are influenced by factors such as the material constant, fractional material, and amplitude.

Vaidya *et al.* [19] investigated the channel flow of MHD Bingham fluid due to peristalsis with multiple chemical reactions, focusing on its application to blood flow through narrow arteries.

Forouzandeh *et al.* [20] conducted a comprehensive review on peristaltic micro pumps. Hussain *et al.* [21] undertook a study to examine the peristaltic motion of a heated couple stress fluid. Their investigation primarily centered on the transportation of gold nanoparticles through coaxial tubes, aiming to explore the potential therapeutic applications for gland tumors and arthritis. In another related study on the peristaltic flow of a heated Jeffrey fluid inside an elliptic duct, Nadeem *et al.* [22] analyzed the streamline behavior. Abd-Alla *et al.* [23] made a numerical solution to study MHD peristaltic transport in a Nano fluid symmetric tube with a porous medium and an inclined wall.

Saffman [24] focused on the mobility of the gas that contains dust components during the initial period. Many researchers have turned to dusty fluids and their applications. According to Manjunatha *et al.* [25], the thermal behavior of conducting dusty fluid flow over a stretching cylinder in a porous medium is influenced by the presence of a non-uniform source or sink. Siddiqa *et al*. [26] looked into the natural convection flow of a dusty fluid in two dimensions. The writers have given a numerical answer to the problem of a dusty boundary layer.

Bilal *et al.* [27] discussed free convective Couette flow of viscoelastic dusty fluid in a rotating frame along with the heat transfer. Khan and Tariq [28] examined the consequences of a porous medium on the behavior of a second-grade fluid, which contains dust particles and exhibits slip effects, in an uneven channel. They mathematically derived a set of nonlinear interconnected equations to describe this complex system. Considering the channel flow of 2nd grade viscoelastic fluid caused by an oscillating wall, Khan *et al.* [29] modeled the phenomena using PDEs while taking into account the impact of mass and heat transfer. Khan *et al.* [30] talked about an analytical solution to a time-fractional magneto hydrodynamic dusty flow of fluid model with variable circumstances. In their study, Khan and Tariq [31] investigated how the peristaltic flow of a Walter's B fluid, which includes dust particles, is influenced by the characteristics of the walls. Their study sheds light on the influence that wall characteristics have on this specific fluid dynamics phenomenon.

Khan and Tariq [32] talked about a 2nd grade investigation in which a granular liquid was moving through a tube with flexible walls which were produced through peristaltic motion. In a dusty nanomaterial for the interaction of a transverse magnetic field that passes over an expanding surface, Mishra *et al.* [33] explored the thermal properties of dust nanoparticles. Ahmed and Rashid [34] explored numerical simulations of a magneto-hydrodynamic convective process occurring within curved channels. Their study focused on examining the behavior of fluid movement and heat transfer under the effect of magnetic fields in such curved

geometries. In order to evaluate the behavior of a dusty flow across a surface, Ali *et al.* [35] looked into the successive over-relaxation (SOR) approach. This work focuses mainly on the dusty flow at convective boundary conditions. In their study on the peristaltic flow of dusty nanofluids, Rashed and Ahmed [36] focused on examining this phenomenon specifically in curved channels. There have been numerous investigations conducted on the numerical simulations of dusty fluid flow. [37]- [46].

Heat transfer is a significant factor in understanding and studying the thermal conduct of fluid systems, including heat transfer in pipes, heat exchangers, boundary layers, and other fluid flow configurations. Engineers and scientists can optimize thermal processes, improve energy efficiency, and design effective heat transfer systems by studying heat transfer in fluid mechanics. Bhatti and Zeeshan [47] conducted an analytical study on the motion of solid elements inside a dusty Jeffery fluid in a planar channel, considering the effects of variable viscosity and heat transfer. The study presented closed-form results for the pressure rise, velocity profile, and temperature profile. It was found that the velocity of fluid varied in the center of the canal due to the influence of variable viscosity, exhibiting contrasting behavior near the walls.

In their study, Hayat *et al.* [48] discussed the influence of thermal radiation on the peristaltic motion of a dusty liquid occurring in a channel with wall characteristics. They also investigated the simultaneous impacts of mass transfer and heat transfer in this system. The research findings contribute to our understanding of the intricate interplay between thermal radiation, peristaltic motion, and the coupled mass transfer and heat phenomena occurring in channels with wall properties.

Ramesh and Devakar [49] examined how transfer of heat affected the peristaltic movement of an incompressible magneto-hydrodynamic fluid from 2nd grade. They found that Increasing the inclination angle leads to higher velocity, temperature, and trapping bolus. This suggests that the channel's angle plays a pivotal role in shaping the fluid’s behavior during peristaltic transport. Nadeem *et al*. [50] considered the impacts of the endoscope on the peristaltic motion of Walter's B fluid. In their study, Hameed *et al.* [51] explored how the peristaltic transport of a second-grade fractional fluid within a tube oriented perpendicularly to the flow is affected by heat transfer and a magnetic field. Their research provides valuable insights into the intricate dynamics of fluid flow and the interplay between magnetic effects, heat transfer, and peristaltic motion in vertical tube configurations.

In their research, Muthuraj *et al.* [52] explored the interrelationship between chemical reactions, wall properties, and the peristaltic transport of a dusty fluid. Their study also

considered the effects of heat and mass transfer, all within the context of magnetohydrodynamics (MHD).Their study sheds light on the intricate dynamics and interplay of these factors in the context of peristaltic flow. Javed and Hayat [53] conducted a study to investigate how transfer of heat affects the peristaltic movement of dusty fluid (using Saffman's Model) in a 2-dimensional channel. They analyzed the influence of different relevant factors on the physical quantities of interest. The study enhances our understanding of how heat transfer influences the behavior of dusty fluid in peristaltic motion, providing valuable insights into this complex system.

The investigation directed by Radhika *et al*. [54] focused to exploring the transfer of heat characteristics within a dusty fluid containing suspended hybrid nanoparticles above a surface undergoing melting. Chinyoka and Makinde [55] studied the heat flow and instability of the fluid movement that contains dust in a canal having different viscosity and electric conductivity. The authors also analyzed the properties of mass, heat, and the flow of fluid by plotting through diagrams. In order to squeeze unsteady Nano fluid movement and transmit heat between the two parallel plates, Singh *et al.* [56] investigated the magnetic field, slip velocity, and mass transfer.

The impact of heat transfer on the peristaltic mechanism of 2^{nd} grade fluid flow through a tube were examined by Hafez *et al*. [57].

Endoscopes are medical instruments used to visualize and inspect the interior of the human body and other porous structures. It is a long, flexible or rigid tube with a camera and light source fixed to its tip.

Endoscopic procedures are commonly used for diagnostic purposes, such as detecting abnormalities, diagnosing diseases, and obtaining tissue samples (biopsies) for further analysis. Few recent studies which are related to peristaltic movement of dusty fluid in an endoscope are following. [58] - [63].

Bhatti *et al.* [64] conducted a study on the heat transfer phenomenon, specifically investigating the influence of nonlinear thermal radiation on the sinusoidal motion of solid magnetic particles within a dusty liquid. The research conducted by Zeeshan *et al.* [65] focused on examining the peristaltic passage of a 3-dimensional bio rheological Casson fluid with magnetic field effects and dust particles in a duct. The findings of their study revealed that the Casson liquid factor amplifies the fluid velocity adjacent to the duct walls while opposing the flow in the centre.

According to Hasona *et al.* [66], the study presented a semi-analytical solution for the MHD peristaltic flowing of a Jeffery fluid considering the existence of Joule's heat effect, employing the multi-step differentially transform approach. Khan *et al.* [67] discussed the Jeffrey liquid

with uniform dust particles in a symmetric channel has recently been studied. Tariq and Khan [68] conducted a study to examine how magneto hydrodynamics affects the peristaltic flow of a dusty fluid within an endoscope. The authors specifically investigated the impact of many constraints, including magnetic field *M*, porous parameter 'α' on the fluid's velocity, pressure rise, and streamlines. In their study, Ramesh and Devakar [69] explored the impact of endoscopes and heat transfer on the peristaltic movement of fluid of a 2^{nd} grade through an inclined tube. The authors specifically noted that the velocity fluid is positively affected by the heat generation parameter.

Das *et al.* [70] investigated the conveyance of blood containing hybrid nanoparticles through an endoscopic annulus featuring elastic walls. Their study considered the influence of electromagnetic forces (EMF) and the presence of blood clotting.

Nadeem *et al.* [71] discussed the entropy interpretation alongside a detailed examination of heat generation. Their study specifically investigated the heated flow within two homocentric curved tubes exhibiting sinusoidal fluctuations. A groundbreaking aspect of their research involves the introduction of a novel peristaltic endoscope inside a curved tube, marking the first instance of such consideration.

In a recent study, Devakar *et al.* [72] examined the implications of magnetohydrodynamics (MHD) on the peristaltic propulsion of a non-Newtonian fluid within a tube that incorporates an endoscope. Das *et al.* [73] conducted a study on simulating the transport of bi-nanoparticles in the bloodstream within an endoscopic canal containing a blood clot under the influence of strong electromagnetic forces.

CHAPTER 3

BASIC LAWS AND CONCEPTS

3.1 Fluid [13]

A fluid is a substance that has the ability to flow and does not possess fixed shape. It is a state of matter that can adapt its shape to fit the container it occupies and can easily deform under the influence of external forces. Fluids encompass liquids and gases, where the particles within them are not rigidly held together and have the freedom to move past one another. The characteristic property of fluids to flow and change shape allows them to exhibit essential properties such as viscosity, density, and pressure.

Viscosity is a property of fluids that characterizes their resistance to flow and is often described as the degree of "thickness" or "stickiness" of the fluid. It is influenced by the internal friction among the particles within the fluid. On the other hand, density refers to the measurement of a fluid's mass per unit volume, indicating the amount of matter packed into a specific space.

Pressure within a fluid refers to the force exerted by the fluid on the surfaces of its container or any objects submerged in it. This force emerges from the interactions between fluid particles and the boundaries they come into a contact with. Pressure can exhibit variability across different points within the fluid, and the analysis of its positional changes falls within the realm of fluid dynamics.

The understanding of fluid behavior holds significant importance in numerous scientific and engineering fields, encompassing disciplines such as physics, chemistry, biology, and fluid mechanics.

Fluids can be classified into different categories based on various criteria. Here are some common classifications of fluids:

3.2 Newtonian and Non-Newtonian Fluids

Newtonian fluids display a linear correspondence between shear stress and shear rate. Examples include water and most common liquids.

Non-Newtonian fluids do not adhere this linear relationship and exhibit more complex behavior. Examples include suspensions, gels, and polymers.

3.3 Compressible and Incompressible Fluids

Compressible fluids, such as gases, can be compressed and their density can change significantly under changes in pressure.

Incompressible fluids, such as liquids, have negligible changes in density even under large changes in pressure.

3.4 Viscous and Inviscid Fluids

Viscous fluids have internal friction or viscosity, which causes resistance to flow and produces shear stress. Liquids are typically viscous.

Inviscid fluids are hypothetical fluids with zero viscosity and do not exhibit internal friction. Ideal gases are often treated as inviscid.

3.5 Single-phase and Multi-phase Fluids

Single-phase fluids exist in a single state, either as a liquid or a gas.

Multi-phase fluids consist of two or more phases coexisting, such as a mixture of liquid and gas, liquid and solid, or gas and solid. Examples include air-water mixture and oil-water emulsion.

3.6 Peristaltic Flow

Peristaltic flow refers to the movement of a fluid through a tube or a channel due to periodic contraction and relaxation of the tube walls. In the context of an endoscope, peristaltic flow is induced by the motion of the endoscope itself or by external forces applied to the tube.

3.7 Second Grade Fluid Model

A second-grade fluid, classified as a non-Newtonian fluid, displays viscoelastic properties. Unlike Newtonian fluids, which have a direct connection between the shear stress and the shear rate, second-grade fluids show a nonlinear relationship between these two parameters. The constitutive equation of a second-grade fluid, which contains higher-order derivatives of the velocity gradient, relates the shear stress to the shear rate. Due to the fluid's elastic properties, this connection is nonlinear. As a result, in addition to the shear rate, the viscosity of a second-grade fluid also depends on the speed of deformation and stress. Second-grade fluid models are used to describe the flow behavior of complex fluids that exhibit viscoelastic properties, such as polymer solutions, certain biological fluids, and some suspensions.

3.8 Dusty Fluid Model

A dusty fluid refers to a fluid in which solid particles are dispersed and interact with the fluid. In the case of a 2nd-grade dusty fluid, in occurrence of solid particles affects the rheological characteristics of the fluid, such as elasticity and viscosity.

3.9 Heat Transfer Mechanisms

The peristaltic flow of a second-grade dusty fluid in an endoscope introduces the possibility of multiple heat transfer mechanisms.

a. Conduction: Heat can be conducted through the endoscope walls, affecting the temperature distribution within the endoscope.

b. Convection: The fluid motion and peristaltic action induce convective heat transfer. This can lead to temperature variations and heat exchange between the fluid and the endoscope walls.

c. Radiation: Depending on the material properties and temperature gradients, radiation heat transfer may also play a vital role in the total heat transfer characteristics.

3.10 Viscous Dissipation

Viscous dissipation occurs as mechanical energy is transformed into thermal energy within a fluid because of internal friction. In the context of peristaltic flow, viscous dissipation accounts for the generation of heat as a result of the fluid's viscosity and the deformation caused by the peristaltic motion.

3.11 Wall Slip

It refers to the phenomenon where a fluid near a solid boundary experiences a reduced effective viscosity and exhibits different flow behavior compared to the bulk fluid. In peristaltic flow within an endoscope, wall slip can influence the fluid dynamics and should be taken into account in the analysis.

3.12 Wave Number

The wave number (δ) can be defined as the relationship between the half-width (radius) of a channel (tube) and the wavelength of a peristaltic wave. It is given by the equation $\delta = \frac{a}{\lambda}$,

where a denotes the characteristic length and λ represents the wavelength.

3.13 Wave Length

The wavelength λ is a fundamental parameter in wave theory that represents the spatial distance between two consecutive identical points on a wave .It finds frequent application in characterizing a range of wave types, encompassing electromagnetic waves, sound waves, and water waves.

Mathematically, it can be written as

$$\lambda = \frac{c}{f},$$

where ,

'c' represents the speed of the wave in the medium. According to the wave equation, as the frequency of a wave increases, the wavelength decreases, and vice versa. This principle remains

valid for numerous wave types, encompassing light waves, sound waves, and water waves. It plays a crucial role in understanding the behavior of waves, such as interference, diffraction, and refraction. It also has significant applications in fields like optics, telecommunications, and many areas of physics and engineering.

3.14 Reynolds Number [56]

The Reynolds number, a dimensionless value, is a vital factor in characterizing fluid flow. It quantifies the balance between inertial and viscous forces within the fluid. In mathematical terms, the Reynolds number *Re* can be represented as:

$$Re = (\rho v d) / \mu$$

where,

ρ denotes the density of the fluid, v represents the velocity of the fluid, d is a characteristic length or linear dimension (such as diameter or radius) in the flow μ stands for the dynamic viscosity of the fluid.

The Reynolds number serves as an indicator of whether a flow is laminar or turbulent. When it is low, the flow tends to be laminar, with viscous forces dominating and the fluid moving in smooth, orderly layers. As the Reynolds number increases, the flow is more likely to transition into a turbulent state, where inertial forces become more prominent, resulting in chaotic and unpredictable fluid motion. It is a crucial parameter in the field of fluid dynamics and finds applications in engineering, physics, and biology. It aids in the analysis and prediction of flow behavior, estimation of pressure drops, evaluation of heat transfer rates, and assessment of fluid flow stability.

3.15 Prandtl Number [57]

The Prandtl number Pr is a dimensionless factor that quantifies the relative significance of momentum diffusion (represented by dynamic viscosity,μ) to thermal diffusion (represented by thermal conductivity,k) in a fluid.

Mathematically, it can be written as

$$Pr = \mu Cp / k \ ,$$

where, μ is the dynamic viscosity of the fluid, which describes its resistance to shear or flow.

Cp represents the specific heat capacity at constant pressure, signifying the quantity of heat energy needed to increase the fluid's temperature. k is the thermal conductivity of the fluid, representing its ability to conduct heat.

The Prandtl number provides valuable insights into the relative efficiency of heat transfer as compared to fluid motion within a system. A higher Prandtl number indicates that momentum diffusion is more dominant than thermal diffusion, resulting in a thicker thermal boundary layer and slower heat transfer. Conversely, a lower Prandtl number suggests that thermal diffusion is more significant, resulting in a thinner thermal boundary layer and more efficient heat transfer.

The Prandtl number is widely used in the analysis and prediction of heat transfer phenomena, especially in convection problems and boundary layer flows. It helps engineers and researchers to understand the behavior of fluids, optimize heat transfer rates, and design efficient thermal systems across various industries and applications.

3.16 Constitutive Equation

A constitutive equation relates the stress tensor to the deformation rate tensor of the fluid. In the case of a second-grade dusty fluid, the constitutive equation accounts for both the viscous behavior of the fluid and the additional stress induced by the suspended particles. This equation helps describe the complex rheological behavior of the fluid.

3.17 Governing Equations for Fluid Motion

The governing equations that describe fluid motion find their basis in upholding the principles of mass, momentum, and energy conservation. These equations describe how the fluid properties, such as velocity, pressure, and temperature, change in response to external forces and internal interactions. The fundamental equations for fluid motion are:

3.18 Continuity Equation

The continuity equation affirms that the mass flow rate entering a control volume equals the mass flow rate exiting the same volume. In the context of peristaltic flow, this equation ensures that the mass flow rate through the endoscope remains constant.

Mathematically, it can be written in the form of

$$\frac{\partial \rho}{\partial t} + \nabla.(\rho V) = 0\,,$$

Where 'ρ' is the density of the fluid, 't' is time, 'v'is the velocity vector, and ∇ denotes the divergence operator. For incompressible fluid above equation can be written as:

$$\nabla.V = 0\,.$$

3.19 Navier-Stokes Equations

Navier-Stokes Equations (Momentum Conservation): The Navier-Stokes equations provide an account of how momentum is conserved within a fluid. These equations consider the impact of fluid viscosity and external forces acting on the fluid. When written differentially, the Navier-Stokes equations take the following form:

$$\partial \frac{\rho v}{\partial t} \frac{\partial(\rho V)}{\partial t} + \nabla \cdot (\rho v v) = -\nabla P + \nabla \cdot \tau + \rho g,$$

where 'P' is the pressure, τ is the stress tensor representing the viscous forces, and g is the gravitational acceleration.

3.20 Energy Equation

The energy equation accounts for the conservation of energy in the system. It incorporates the effects of heat transfer, including conduction, convection, and radiation. In the case of peristaltic flow in an endoscope with must viscous dissipation, the energy equation would consider the heat generated by viscous dissipation and its effect on the temperature distribution. In differential form, the energy equation can be formulated as:

$$\rho c \frac{\partial T}{\partial t} + \rho(\boldsymbol{u} \cdot \nabla)T = k\nabla^2 T + \eta\left(\frac{\partial u_i}{\partial x_j} + \frac{\partial u_j}{\partial x_i}\right)^2 + Q_r\,,$$

where

ρ is the fluid density,

c is the specific heat capacity,

T is the temperature,

$\boldsymbol{u}$ represents the velocity vector of the fluid,

k is the thermal conductivity,

η is the dynamic viscosity,

$\frac{\partial T}{\partial t}$ is the time derivative of temperature ,

Q_r represents the heat generated by viscous dissipation.

3.21 Boundary Conditions

Appropriate boundary conditions be defined to simulate the peristaltic flow in an endoscope. These conditions may include prescribed wall motions, inlet and outlet boundary conditions, and appropriate conditions for the fluid-solid interface to capture the effects of particle adhesion or slippage.

3.22 Surface Forces

Surface forces are the forces exerted on the fluid at the interface between the fluid and the system boundaries, like the endoscope walls. These forces arise due to the interaction between the fluid and the solid surfaces, encompassing effects such as viscous forces, pressure forces, and other forces resulting from fluid-wall interactions. These surface forces significantly impact the flow behavior, fluid deformation, and the resultant peristaltic motion observed in the system.

3.23 Body Forces

The forces acting on the entire volume of the fluid, extending beyond its boundaries. These forces originate from external factors or physical phenomena, including gravity,

electromagnetic forces, or other relevant influences. In the scenario of peristaltic movement of a 2nd-grade dusty fluid in an endoscope with viscous dissipation, body forces may include gravity forces and other forces that are pertinent to the particular system being studied. These body forces contribute to the overall flow behavior, pressure distribution, and fluid deformation observed in the system.

3.24 Thermal Conductivity

Thermal conductivity, represented by κ, is an essential material property that measures a substance's ability to conduct heat. It characterizes the effectiveness of heat transfer within the material concerning the temperature gradient and the surface area. In the particular context of analyzing the peristaltic transport behavior of a second-grade dusty fluid in a tube while considering heat transfer effects, the thermal conductivity of the fluid plays a critical role. It plays a crucial role in shaping the efficiency of heat transfer between the fluid and the tube walls, establishing the temperature profile within the fluid, and controlling overall thermal characteristics of the system. The thermal conductivity affects important aspects such as heat conduction, the development of thermal boundary layers, and the dissipation of heat generated by viscous effects within the fluid. Accurate consideration and understanding of the thermal conductivity of the second-grade dusty fluid are indispensable for analyzing and predicting heat transfer dynamics, as well as optimizing the design and performance of such systems.

3.25 Specific Heat Capacity

The specific heat capacity, represented by either C or Cp, is a crucial thermodynamic parameter that measures the quantity of heat energy needed to increase the temperature of a specified amount of the second-grade dusty fluid by one degree. Specifically, it measures the fluid's ability to store and exchange thermal energy. By understanding the specific heat capacity, we gain insights into the fluid's heat absorption or release as its temperature changes. This property plays a critical role in comprehensively analyzing the dynamics of heat transfer, temperature distribution, and overall thermal behavior of the fluid within the tube during peristaltic transport. The specific heat capacity influences the fluid's thermal response to variations in the surrounding environment and significantly impacts temperature profiles and energy exchange throughout the transport process. Accurate consideration of the specific heat capacity of the

second-grade dusty fluid is therefore vital for predicting heat transfer characteristics as well as optimizing system design and performance.

3.26 Stream Function

The stream function, denoted as ψ, serves as a mathematical tool used for the characterization and examination of the flow dynamics within an endoscope system where a second-grade dusty fluid is subjected to peristaltic flow, taking into account the effects of viscous dissipation. By definition, the stream function is a scalar field that provides valuable insights into the motion of the fluid. It aids in visualizing the flow patterns and understanding the direction and magnitude of fluid movement. The streamlines, which are imaginary lines tangential to the velocity vectors at each point, can be determined from the stream function. By calculating and visualizing the streamlines, one can grasp the flow characteristics, including the formation and propagation of pressure waves, flow reversal, and the complex interplay between fluid mechanics, viscous dissipation, and heat transfer. Moreover, the stream function allows for the determination of important transport properties, such as the mass flow rate and shear stress distribution. Incorporating the stream function analysis into the study of peristaltic flow in an endoscope with viscous dissipation enhances our understanding of the fluid's behavior, facilitating the design, optimization, and prediction of the system's performance.

3.27 Streamlines

Streamlines are visual representations of the flow direction and pattern within a fluid system. They depict the paths that fluid particles would follow as they traverse through the flow field. Each point along a streamline indicates the instantaneous fluid velocity vector at that specific point.

Mathematically, streamlines are curves that coincide with the orientation of the velocity vector field at every single point along their path. These curves illustrate the paths that individual fluid particles would take without crossing or mixing with one another. Streamlines never intersect, maintaining their integrity throughout the flow field.

Streamlines are valuable tools for visualizing and comprehending flow behavior in various fields, including fluid dynamics, aerodynamics, and heat transfer. They provide insights into flow patterns, areas of separation, and regions of recirculation within the fluid. Analyzing

streamlines facilitates a deeper understanding of the overall flow structure, enables the identification of regions with varying velocities, and aids in assessing the influence of obstacles or boundary conditions on fluid flow.

3.28 Similarity Transformation

A similarity transformation is a mathematical approach utilized to simplify the analysis of a physical system by converting the governing equations into a dimensionless form. It involves rescaling variables and parameters to eliminate the influence of specific dimensions or units, thus revealing underlying relationships and behaviors that are independent of system size or units. By introducing dimensionless variables and parameters, the complexity of the problem is reduced, enabling a more general analysis that can be applied across different scales or conditions. The application of similarity transformations aids in streamlining the mathematical formulation, identifying dimensionless groups and relationships, and recognizing dominant physical phenomena. This technique finds broad application in diverse scientific and engineering fields to extract fundamental principles and facilitate comparisons between various systems or conditions.

3.29 Perturbation Technique

Perturbation technique is a mathematical method used to approximate the solution of a problem by introducing small parameter variations or perturbations into the governing equations. It is commonly employed when an exact analytical solution is difficult or impossible to obtain, and provides an approximate solution by expanding the unknown variables in a power series utilizing small parameter. By applying perturbation technique to the governing equations describing the peristaltic motion of a 2^{nd} grade dusty fluid, the problem can be simplified and approximate solutions can be obtained. Perturbation analysis involves expanding the unknown variables, such as velocity and pressure, in a power series of a small parameter, typically associated with the amplitude or wavelength of the peristaltic wave. The series is then truncated at a certain order, neglecting higher-order terms, and the resulting approximate equations can be solved to obtain solutions that provide insights into the flow behavior.

CHAPTER 4

PERISTALTIC FLOW OF A DUSTY ELECTRICALLY CONDUCTING FLUID THROUGH A POROUS MEDIUM IN AN ENDOSCOPE

4.1 Introduction

In this chapter we have reviewed the paper of Tariq and Khan [68] with the title “Peristaltic movement of an electrically conductive dusty fluid within an endoscope through a porous medium." This research investigates how Magnetohydrodynamics (MHD) influences the movement of a dusty fluid during peristaltic motion within an endoscope. The experiment involves a setup with concentric tubes containing an incompressible fluid flowing through a porous material. Notably, the inner tube remains rigid, while the outer tube can flex. To understand this complex system, the study formulates governing equations for both the solid granules and the fluid, considering conditions of long wavelengths and low Reynolds numbers. The outcomes of this investigation are presented through graphical representations, offering insights into how different factors impact velocity, pressure changes, and the flow patterns. One of the primary findings is that the trapped bolus, which refers to a mass of food or fluid undergoing peristaltic motion, exhibits a reduction as the parameter α decreases. Conversely, it increases as the parameter M, representing the strength of the magnetic field, increases.

4.2 Mathematical Formulation

In this study, the research focuses on the flow of a viscous and dusty incompressible fluid through a co-axial tube configuration. The region between the inner and outer tubes is entirely filled with this dusty fluid. To add complexity to the setup, a uniform magnetic field, denoted

as B_0, is applied, which causes the fluid to become electrically conductive. It's crucial to emphasize that, under conditions marked by lower magnetic Reynolds numbers, the influence of the induced magnetic field can be neglected. To analyze and understand this intricate fluid dynamics problem, the researchers use cylindrical polar coordinates (R, Z) to denote the radial and axial positions within the tubes, where R represents the radial distance from the center, and Z denotes the position along the tube's centerline. Mathematically, two walls can be given as

$$r_1 = a_1\,, \tag{4.1}$$

$$r_2 = a_2 + b\sin\frac{2\pi}{\lambda}(z - ct), \tag{4.2}$$

where a_1 is the radius of the inner tube and a_2 is outer tube's radius, c denotes wave speed, the time is represented by t, and b is the amplitude, wavelength are denoted by λ. In order to maintain a steady flow, the following transformation has been considered.

$$V = v + c, U = u, R = r, Z = z + ct, \tag{4.3}$$

where (U, V) refer to velocities in the laboratory frame, while (u, v) correspond to velocities in the wave frame. The governing equations for the dusty MHD fluid and the motion of dust granules passing through a porous tube are provided as follows:

$$\frac{\partial v}{\partial z} + \frac{u}{r^2} + \frac{\partial u}{\partial r} = 0, \tag{4.4}$$

$$\rho\left(u\frac{\partial u}{\partial r} + v\frac{\partial u}{\partial z}\right) = \mu\left(\frac{\partial^2 u}{\partial r^2} + \frac{\partial^2 y}{\partial z^2} - \frac{u}{r^2} + \frac{1}{r}\frac{\partial u}{\partial r}\right) - \frac{\partial p}{\partial r} - \frac{\mu\phi}{k}u + Lr^*(u_p - u), \tag{4.5}$$

$$\rho\left(u\frac{\partial v}{\partial r} + v\frac{\partial v}{\partial z}\right) = \mu\left(\frac{\partial^2 v}{\partial r^2} + \frac{\partial^2 v}{\partial z^2} + \frac{1}{r}\frac{\partial v}{\partial r}\right) - \frac{\partial p}{\partial z} + Lr^*(v_p - v) - \left(\sigma B_0^2 + \frac{\mu\phi}{k}\right)(v + c), \tag{4.6}$$

$$\frac{\partial v_p}{\partial z} + \frac{u_p}{r^2} + \frac{\partial u_p}{\partial r} = 0, \tag{4.7}$$

$$\rho\left(u_p\frac{\partial u_p}{\partial r} + v_p\frac{\partial v_p}{\partial z}\right) = \frac{r^*}{m}(u - u_p) - \frac{\partial p}{\partial r}\,, \tag{4.8}$$

$$\rho\left(u_p\frac{\partial v_p}{\partial r} + v_p\frac{\partial v_p}{\partial z}\right) = \frac{r^*}{m}(v - v_p) - \frac{\partial p}{\partial z}\,. \tag{4.9}$$

The parameters in the equations include the fluid density denoted as ρ, pressure represented as p, the magnetic field strength as B_0, the resistance coefficient for solid particles as r^*, fluid's electric conductivity as σ, and the porosity and permeability denoted as ϕ and k, respectively.

The number density of the dust granules is assumed to remain constant and is represented by the symbol L. The following boundary conditions are given below as:

$v = -c\,, u = 0\,,$ at $r = r_1\,,$ (4.10)

$v = -c\,,$ at $r = r_2 = a_2 + b\sin\frac{2\pi}{\lambda}z\,.$ (4.11)

The dimensionless quantities that have been incorporated into the analysis are as follows.

$\overline{r} = \frac{r}{a_2}\,, \overline{r_1} = \frac{r_1}{a_2} = \frac{a_1}{a_2} = \varepsilon < 1, \overline{z} = \frac{z}{\lambda}\,, \overline{p} = \frac{a^2 p}{\lambda\mu c}\,, \overline{v} = \frac{v}{c}\,, \frac{1}{\alpha} = \frac{\phi\, a_2^2}{k}, \overline{u} = \frac{u}{\delta c}\,, \delta = \frac{a_2}{\lambda}\,, \theta = \frac{b}{a_2}\,, \overline{r_2} = \frac{r_2}{a_2} = 1 + \theta\sin 2\pi z\,, M^2 = \frac{\sigma B_0^2 a_2^2}{\mu}\,.$ (4.12)

Assuming long wavelengths and a low Reynolds number, the system of equations is provided below after eliminating the bar.

$\frac{\partial v}{\partial z} + \frac{u}{r^2} + \frac{\partial u}{\partial r} = 0,$ (4.13)

$\frac{dp}{dr} = 0,$ (4.14)

$\frac{dp}{dz} = A\left(v_p - v\right) + \frac{1}{r}\frac{\partial v}{\partial r} + \frac{\partial^2 v}{\partial r^2} - \eta^2(v + 1),$ (4.15)

$\frac{dp}{dz} = B\left(v - v_p\right),$ (4.16)

where $A = \frac{Lr^* a_2^2}{\mu}\,, B = \frac{r^* a_2}{mc}\ \ and\ \eta^2 = \frac{1}{a} + M^2,$

with boundary conditions:

$v = -1\,, u = 0$ at $r = r_1\,,$ (4.17)

$v = -1$ at $r = r_2 = 1 + \theta\, sin\, 2\pi z\,.$ (4.18)

For the laboratory frame, the rate of flow is specified by:

$\theta = 2\pi\int_{r_1}^{r_2} VR\, dR\,.$ (4.19)

Using equation (4.3) and integrating equation (4.18), it becomes

$\theta = q + \pi c(r_2^2 - r_1^2)\,.$ (4.20)

In the wave frame, the flow rate is designated as $'q'$ and is articulated as follows:

$$q = 2\pi \int_{r_1}^{r_2} vr\, dr. \tag{4.21}$$

The time averaged flow rate is

$$\overline{Q} = \frac{1}{T}\int_0^T \theta\, dt. \tag{4.22}$$

Substituting equation (4.20) into equation (4.22) and performing integration, the result is

$$\overline{Q} = q + \pi c\left(a_2^2 - a_1^2 + \frac{b^2}{2}\right). \tag{4.23}$$

Equation (4.23) becomes

$$Q = F + \frac{1}{2}\left(1 - \varepsilon^2 + \frac{\theta^2}{2}\right), \tag{4.24}$$

where $Q = \frac{\overline{Q}}{2\pi a_2^2 c}$, $F = \frac{q}{2\pi a_2^2 c}$.

The nondimensional volume flow rate is:

$$F = \int_{\overline{r}_1}^{\overline{r}_2} \overline{r}\,\overline{v}\, dr. \tag{4.25}$$

Equations (4.14) and (4.15) are solved w.r.t boundary conditions Equation (4.16) and (4.17) as a modified Bessel equation, to obtain the solution as

$$v(r,z) = C_1 J_0(\eta r) + C_2 K_0(\eta r) - \frac{1}{\eta^2}\left(\left(\frac{A}{B} - 1\right)\frac{dp}{dz} + \eta^2\right). \tag{4.26}$$

The modified Bessel functions of the first and second types are represented as J_0 and K_0, respectively. Also,

$$C_1 = \frac{(K_0(\eta\varepsilon) - K_0(\eta r_2))(\frac{A}{B} - 1)\frac{dp}{dz}}{\eta^2(J_0(\eta r_2)K_0(\eta\varepsilon) - J_0(\eta\varepsilon)K_0(\eta r_2))}, \tag{4.27}$$

$$C_2 = \frac{(J_0(\eta r_2) - J_0(\eta\varepsilon))(\frac{A}{B} - 1)\frac{dp}{dz}}{\eta^2(J_0(\eta r_2)K_0(\eta\varepsilon) - J_0(\eta\varepsilon)K_0(\eta r_2))}\ . \tag{4.28}$$

The formula describing $\frac{\mathrm{dp}}{\mathrm{dz}}$ is:

$$\frac{dp}{dz} = (\frac{A}{B} - 1)^{-1}(\eta^4(r_2^2 + 2F - \varepsilon^2)\big(J_0(\eta r_2)K_0(\eta\varepsilon) - J_0(\eta\varepsilon)K_0(\eta r_2)\big))(-\eta^2 r_2^2 J_2(\varepsilon r_2)K_0(\eta\varepsilon) - \varepsilon^2\eta^2 J_2(\varepsilon\eta)K_0(\eta r_2) + \eta^2 r_2^2 J_0(\varepsilon\eta)K_2(\eta r_2) + \varepsilon^2\eta^2 J_0(\eta r_2)K_2(\eta\varepsilon) - 4)^{-1}. \tag{4.29}$$

For velocity of solid particles can be obtained by using:

$$v_p(r,z) = v(r,z) - \frac{1}{B}\frac{dp}{dz} \tag{4.30}$$

Graphs

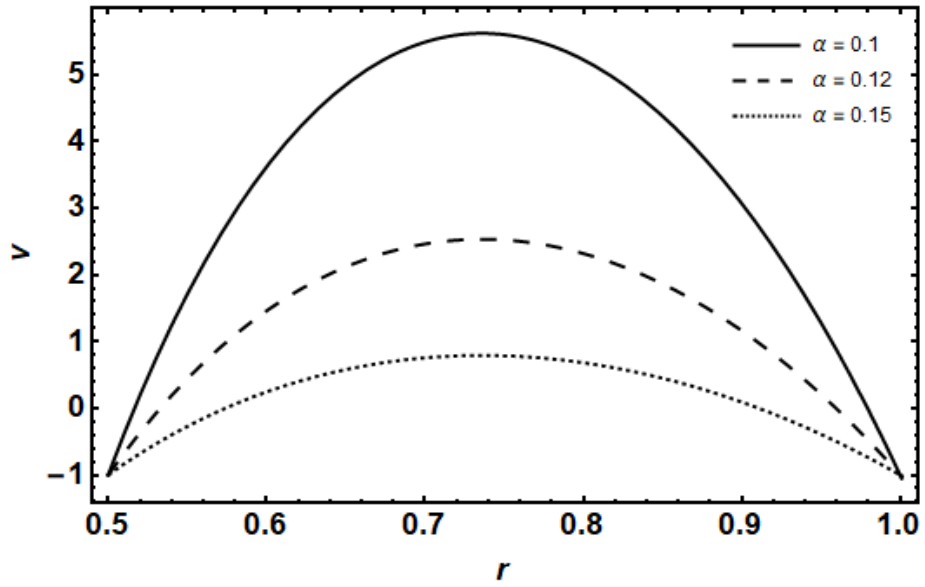

Figure 4.1: Velocity profile of the fluid for various values of α with $M = 0.4, \theta = 0.8, A = 2, B = 2, \varepsilon = 0.5, Q = 0.9$.

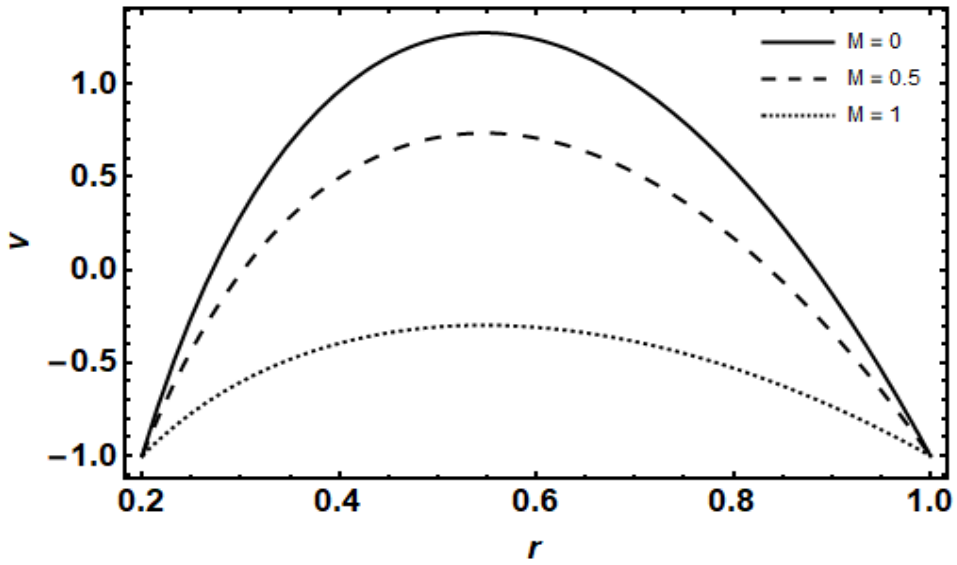

Figure 4.2: The velocity profile of the fluid for various values of M with $\alpha = 0.4, \theta = 0.4, A = 2, B = 1.5, \varepsilon = 0.2, Q = 0.9$.

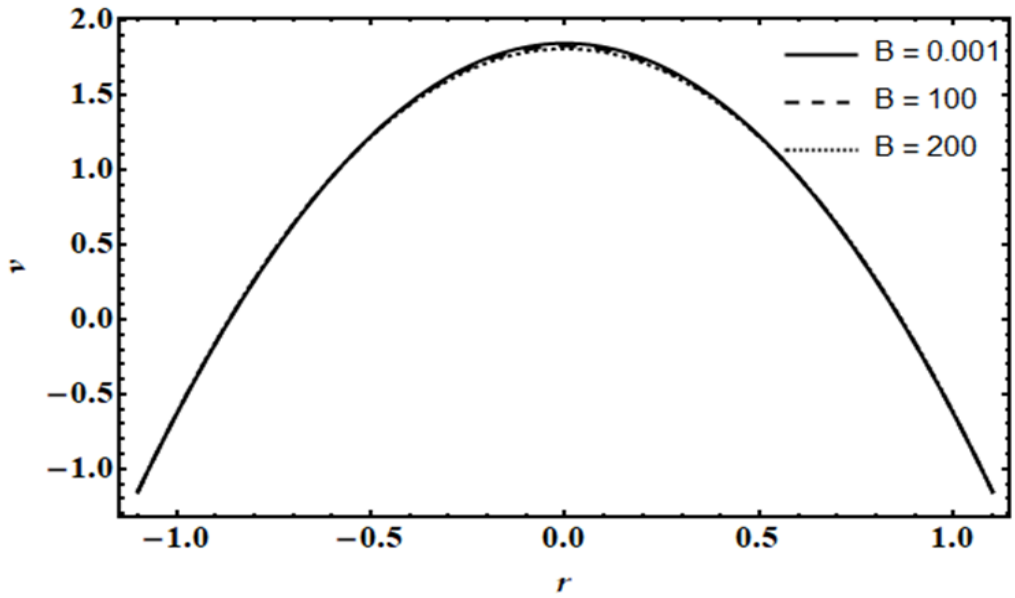

Figure 4.3: The velocity profile of the fluid for various values of B with $\alpha = 0.4, \theta = 0.4, A = 2, M = 0.5, \varepsilon = 0.2, Q = 0$

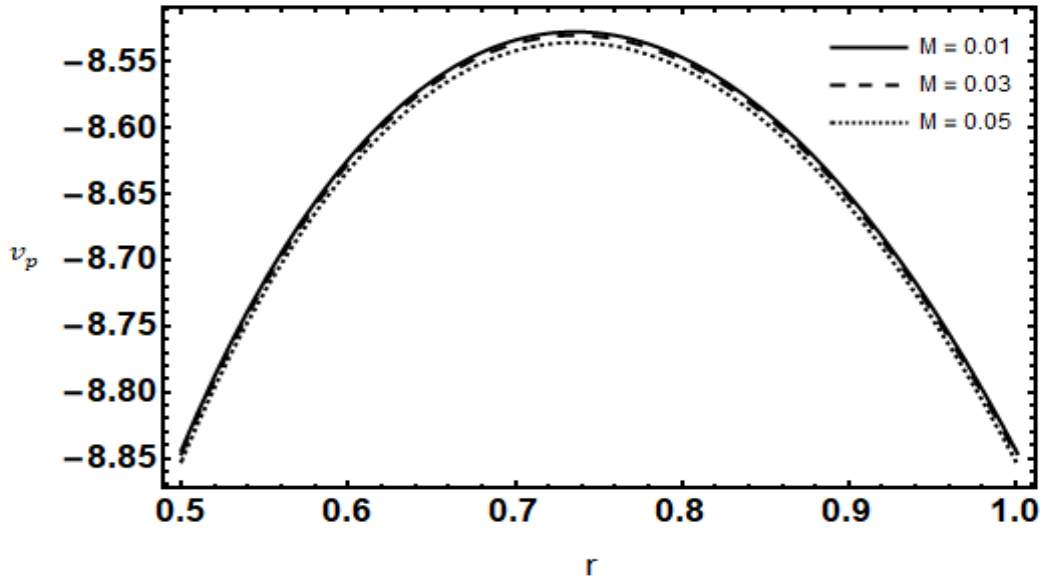

Figure 4.4: The velocity profile of the solid particles for various values of M with $\alpha = 0.15, \theta = 0.8, A = 2, B = 2.5, \varepsilon = 0.5, Q = 0.3$.

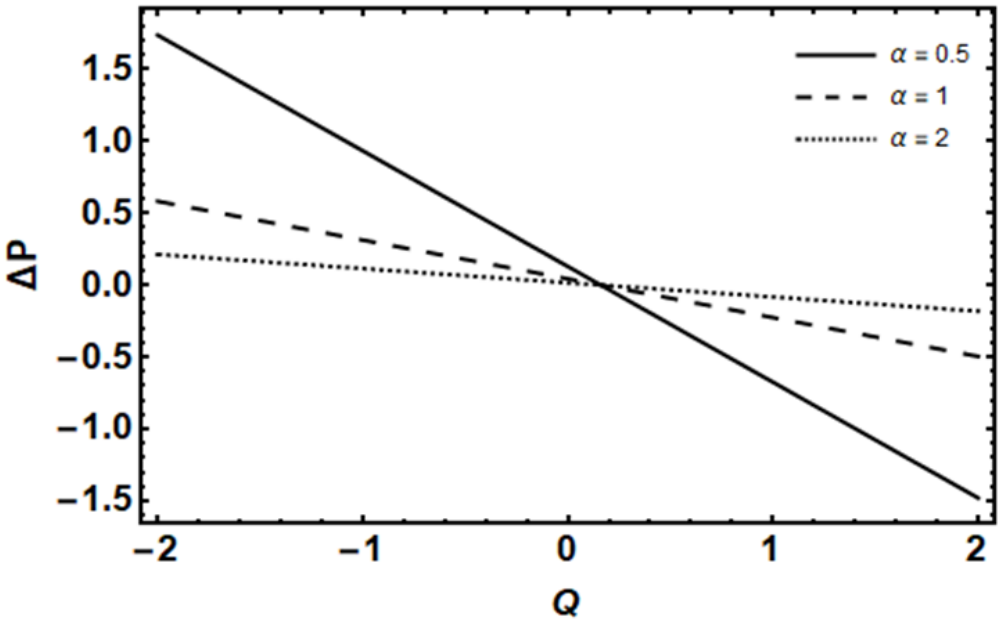

Figure 4.5: The pressure rise for several of α with $\varepsilon = 0.4, \theta = 0.8, A = 2, B = 0.2, M = 0.4$.

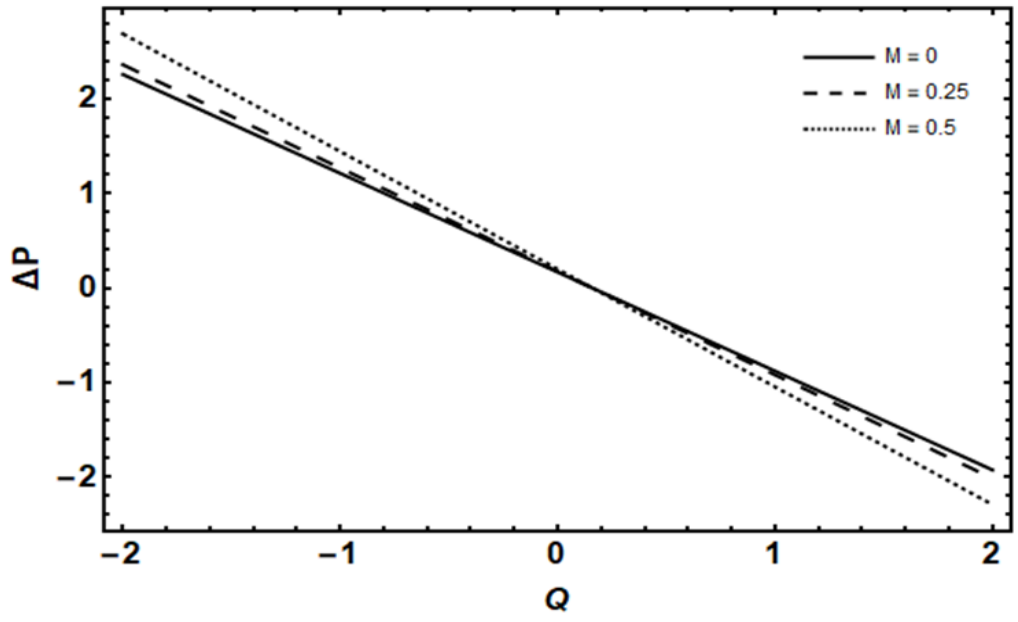

Figure 4.6: The pressure rise for various values of M with $\alpha = 0.4, \theta = 0.8, A = 2, B = 0.2, \varepsilon = 0.5$.

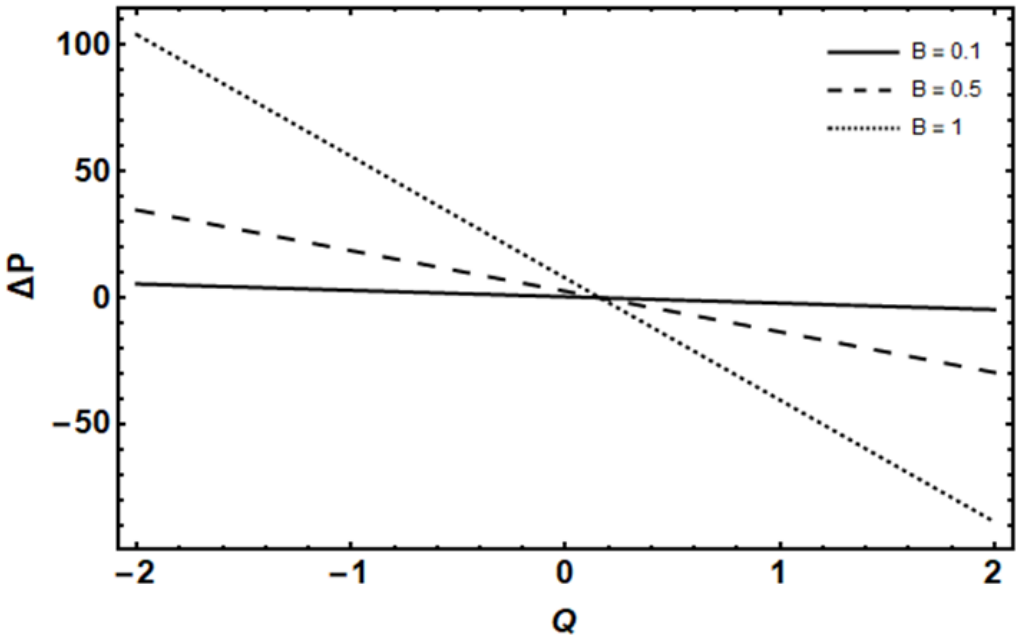

Figure 4.7: The pressure rise for various values of B with $\alpha = 0.4, \theta = 0.8, A = 2, M = 0.5, \varepsilon = 0.2$

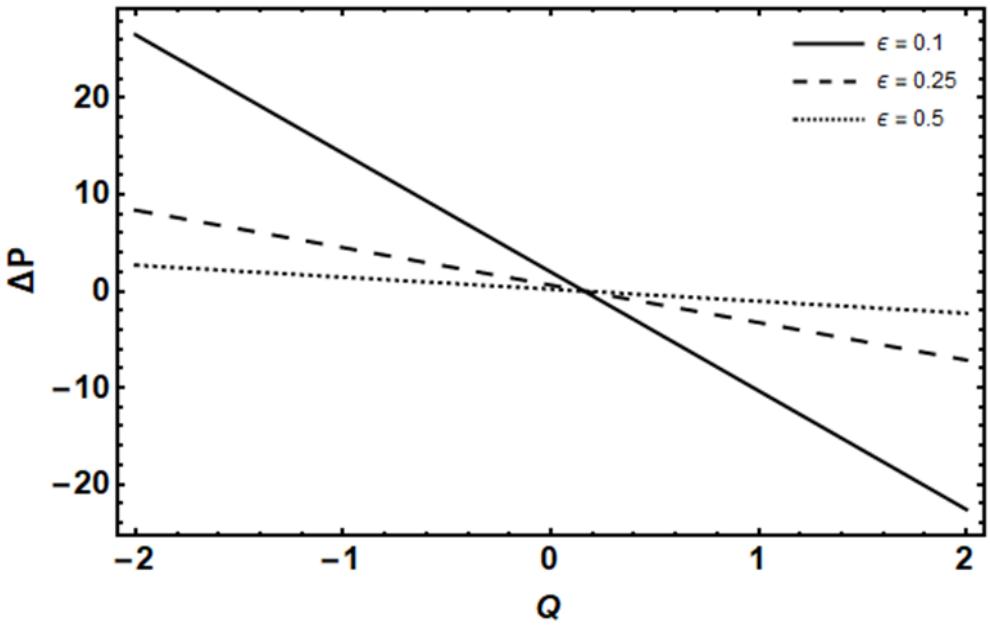

Figure 4.8: The pressure rise for various values of ϵ with $\alpha = 0.4, \theta = 0.8, A = 2, B = 0.2, M = 0.5$.

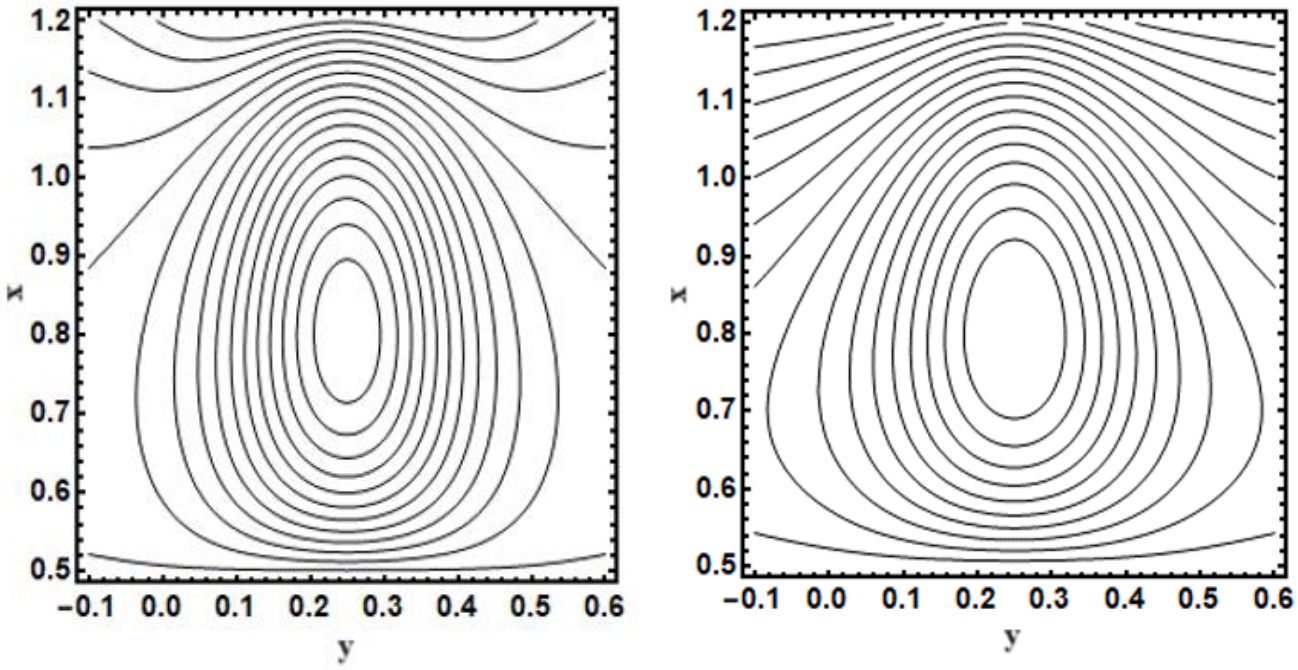

$(i)\ \alpha = 0.1$

$(ii)\ \alpha = 0.2$

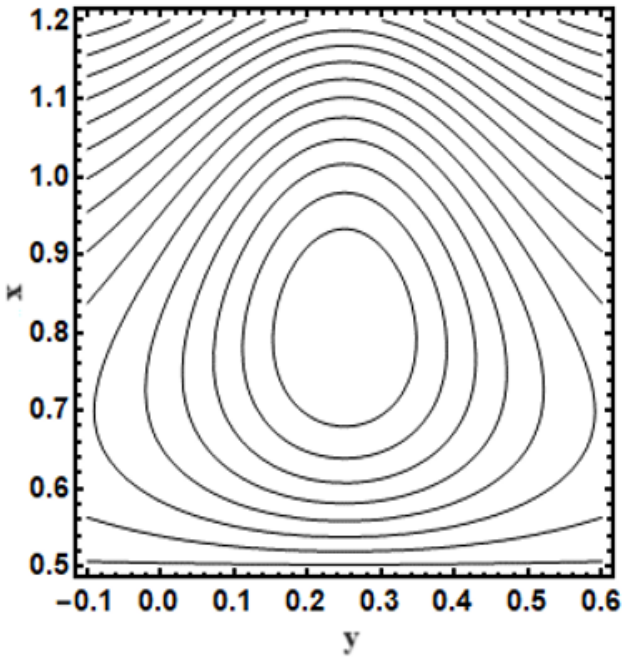

$(iii)\ \alpha = 0.4$

Figure 4.9: Contour graphs of the fluid for various values of α with $M = 0.5, \theta = 0.15, A = 2, B = 3, \varepsilon = 0.5, Q = 1.5$.

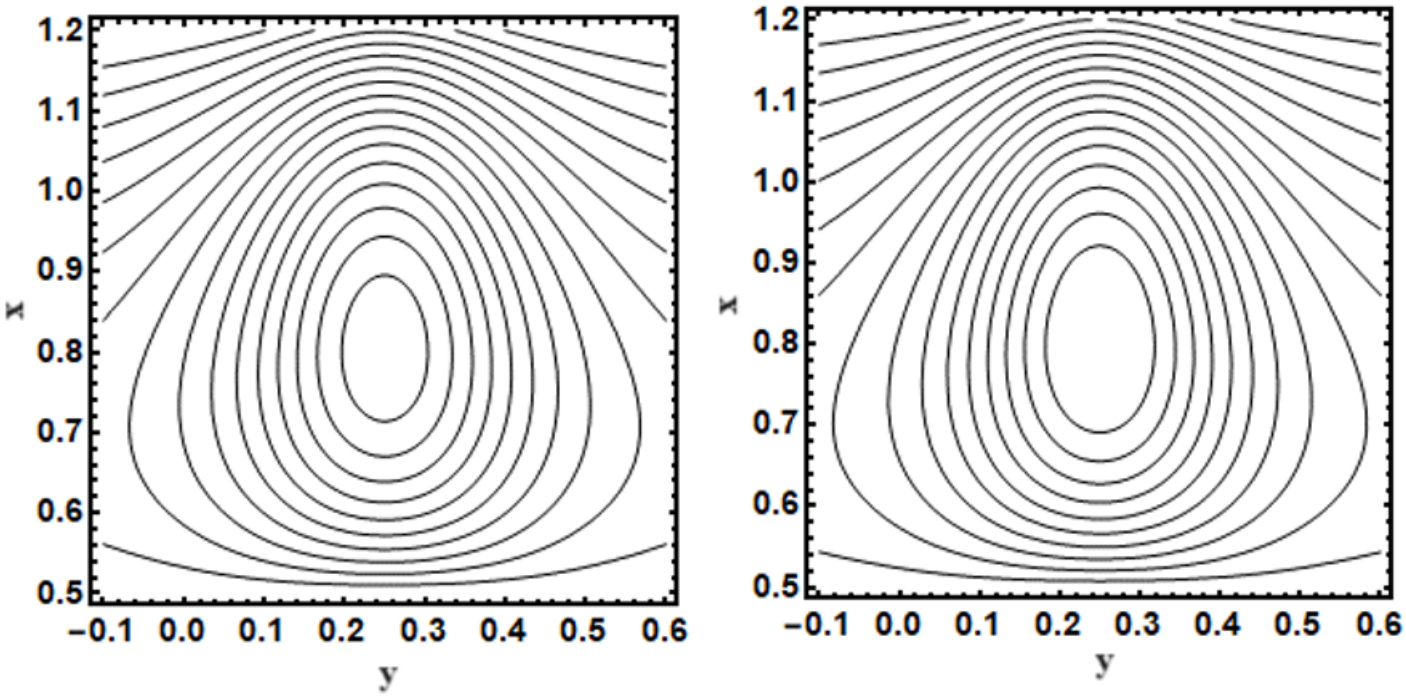

$(i)\ M = 0$ $(ii)\ M = 0.5$

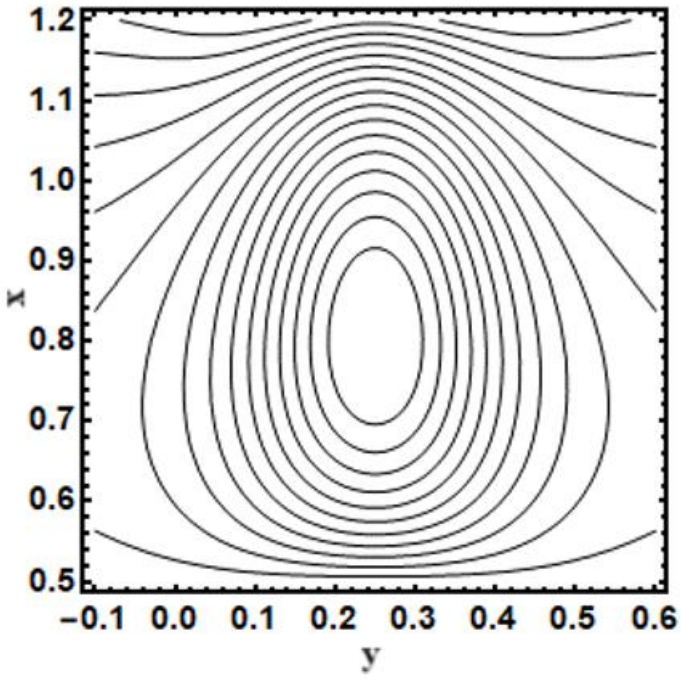

$(iii)\ M = 1.5$

Figure 4.10: Contour graphs of the fluid for various values of M with $\alpha = 0.2, \theta = 0.15, \mathrm{A} = 2, \mathrm{B} = 3, \varepsilon = 0.5, \mathrm{Q} = 1.5$.

4.3 Discussion

To validate the accuracy of the analytical findings, we also visually represented them through graphs to assess how various parameters affect the velocity, pressure rise, and streamline patterns of the granular fluid. Figures 4.1 and 4.2 provide a visual representation of how two critical factors, namely the porosity parameter (α) and the magnetic field strength (M), impact the velocity of the dusty fluid. The porous surface serves as an effective resistance force due to its efficient fluid absorption capabilities.

In figure 4.1, we can observe that as the porosity parameter (α) rises, there is a corresponding reduction in the velocity of the dusty fluid. This decline in velocity can be attributed to the increased porosity parameter, indicating an improved capacity of the passage to absorb the fluid. Consequently, this heightened fluid absorption leads to a decrease in velocity. In figure 4.2, we see a clear relationship between the Hartmann number, denoted as M, and velocity. As M increases, there is a corresponding decrease in fluid velocity. This phenomenon occurs because the heightened electromagnetic force introduces friction, which ultimately results in a noticeable decrease in the fluid's velocity. Additionally, as the concentration parameter (B) rises, figure 4.3 illustrates a decrease in velocity. The increasing concentration parameter corresponds to a diminishing velocity. In figure 4.4, the ascent in magnetic force results in the descent of solid particles. Figure 4.5 illustrates the influence of α on pressure rise. It is evident that enhanced pumping occurs within the range of $0.1 < Q < 2$. At $Q = 0.1$, there is no pumping. With higher values of the porous parameter, the range within which peristaltic pumping is effective widens. Furthermore, an increase in the porous parameter leads to a reduction in pressure rise, indicating that as the porous parameter increases, the pressure rise decreases. Figure 4.6 displays the variation in fluid pressure resulting from changes in the Hartman number (M). Increasing the magnetic field strength (M) results in a corresponding increase in pressure within the pumping region. Consequently, raising the Hartman number implies the need for additional pressure to facilitate fluid pumping. Figure 4.7 represents the impact of the concentration parameter (B). When the concentration parameter increases, it signifies a higher concentration of solid particles suspended in the fluid. Consequently, increased pressure becomes essential to pump the fluid within the pumping region. ϵ, denoting the radius ratio of the tube, is a key factor to consider. When ε is increased, it leads to a decrease in fluid pressure.

Figure 4.8 graphically illustrates how the increase in ϵ acts as a counterinfluence on pressure, causing it to decrease.

The streamline patterns for the porous parameter and Hartmann number can be observed in Figures 4.9 and 4.10. In Figure 4.9, the streamlines reveal the impact of porous parameters. It can be concluded that as porosity increases, the trapped bolus expands and is pushed outward. This suggests that the fluid's motion becomes more uniform as the bolus expands. When considering the magnetic parameter (M), it becomes clear that the trapped bolus experiences a decrease in size. This signifies that the fluid's behavior becomes more complicated due to the resistance introduced by the magnetic parameter within the flow. By focusing on the pumping regions in these figures, we can better understand how various parameters affect pressure rise and fluid movement in the respective systems described.

4.4 Conclusion

The present analysis focuses on the peristaltic flow of a dusty fluid within a porous annulus. It has yielded exact solutions for both the pressure gradient and axial velocity. Key conclusions derived from this analysis include the following:

The velocity of the dusty fluid flowing through an endoscope experiences a decrease due to the influence of the porous parameter and the magnetic field. Additionally, an increase in pressure is noted when considering the magnetic parameter (M) and the concentration parameter (B). These parameters stimulate the activity of the wall, contributing to heightened pressure within the system.As the porous parameter increases, the trapped bolus expands, leading to smoother fluid flow within the system.Conversely, an increase in the magnetic parameter (M) results in the compression of the trapped bolus with in the pumping region. The magnetic field parameter functions as a frictional force on the flowing fluid, leading to an impact on the fluid's flow dynamics. Consequently, this frictional effect causes the trapped bolus to contract.

CHAPTER 5

PERISTALTIC FLOW OF A SECOND GRADE DUSTY FLUID IN AN ENDOSCOPE WITH VISCOUS DISSIPATION

5.1 Introduction

This chapter extends the work of Tariq and Khan [68] by incorporating the impact of viscous dissipation into the study of peristaltic flow within an endoscope for a second-grade dusty fluid. The problem is modeled by assuming axial symmetric 2 dimensional channel, constant number density of solid particles and also consider cylindrical coordinate systems along the radial and axial direction. The coupled differential equation has been modeled by using perturbation technique to find the exact solution. Also used Mathematica software to find the numeric solutions of coupled equations. The impact of various parameters are discussed.

5.2 Mathematical Formulation

Consider an axial symmetric 2-dimensional channel of the peristaltic movement of a 2nd grade fluid containing dust particles in an endoscope. A solid particles are equal in sizes with number density further, assuming that the radial and axial directions of the cylinder's coordinates, R and

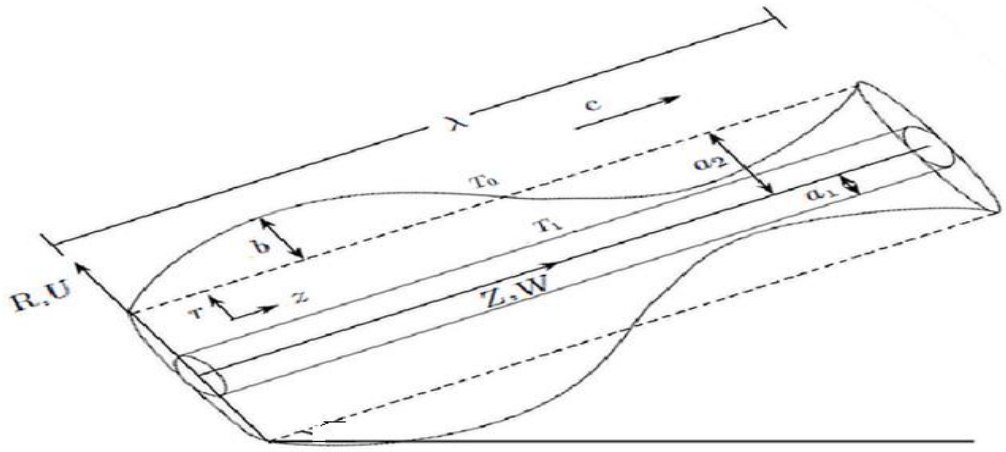

Figure 5.1: Geometry of the problem

Z, respectively, are along its radial and axial axes. The geometry of wall surfaces are defined n the figure 5.1 and the equations of geometry are defined in previous equations (4.1) and (4.2). The fundamental equations that govern the problem are provided as follows:

$$div\,\overline{\boldsymbol{V}} = 0\,, \tag{5.1}$$

$$\rho\frac{d\overline{\boldsymbol{V}}}{d\bar{t}} = div\,\overline{\boldsymbol{S}} + \rho\overline{\boldsymbol{b}} + KN\left(\overline{\boldsymbol{V}}_{\boldsymbol{s}} - \overline{\boldsymbol{V}}\right), \tag{5.2}$$

where ρ is the density, $\rho\overline{\boldsymbol{b}}$ represent the body force, K is the coefficient of resistance, and N is the number density of solid particles.

$$\frac{\partial\overline{\boldsymbol{V}}_{\boldsymbol{s}}}{\partial\bar{t}} + \overline{\boldsymbol{V}}_{\boldsymbol{s}}(\overline{\boldsymbol{V}}.\overline{\boldsymbol{V}}_{\boldsymbol{s}}) = \frac{K}{m}\left(\overline{\boldsymbol{V}} - \overline{\boldsymbol{V}}_{\boldsymbol{s}}\right), \tag{5.3}$$

where $\overline{\boldsymbol{V}}_{\boldsymbol{s}}$ the velocity of solid particles, K is is the coefficient of resistance, m is the mass of the solid particles.

$$\rho c_p\left(\frac{\partial\bar{T}}{\partial\bar{t}} + (\overline{\boldsymbol{V}}.\overline{\boldsymbol{V}})\overline{T}\right) = \kappa(\overline{\boldsymbol{V}}^2\overline{T}) - \boldsymbol{\tau}.(\boldsymbol{grad}\,\overline{\boldsymbol{V}}), \tag{5.4}$$

where

$\bar{T}$ is the temperature , c_p is the specific heat capacity at constant press, κ is the thermal conductivity and $\boldsymbol{\tau}$ is the Cauchy stress tensor.

The constitutive relation for the stress tensor in a second-grade fluid can be expressed as:

$$\overline{S} = -\overline{P}I + \overline{\boldsymbol{\tau}}, \tag{5.5}$$

$$\overline{\boldsymbol{\tau}} = \mu\overline{A}_1 + \alpha_1\overline{A}_2 + \alpha_2(\overline{A}_1)^2, \tag{5.6}$$

where $\overline{\boldsymbol{\tau}}$ is the extra stress tensor, μ is the coefficient of viscosity and α_1 and α_2 are material constants. $\overline{A}_1$ and $\overline{A}_2$ are kinematic tensors can be formulated as

$$\overline{A}_1 = (\text{grad}\ \overline{\mathbf{V}}) + (\text{grad}\ \overline{\mathbf{V}})^{\mathbf{t}}, \tag{5.7}$$

$$\overline{A}_2 = \frac{d\overline{\mathbf{A}_1}}{d\bar{t}} + \overline{A}_1(\text{grad}\,\overline{\mathbf{V}}) + (\text{grad}\,\overline{\mathbf{V}})^t\,\overline{A}_1\,. \tag{5.8}$$

where $\overline{\mathbf{V}} = (\overline{U},\overline{W})$

The equations that govern the system in the fixed frame (R, Z) can be formulated as follows:

$$\rho\left[\overline{U}\frac{\partial\overline{U}}{\partial\overline{R}}+\overline{W}\frac{\partial\overline{U}}{\partial\overline{Z}}\right]==-\frac{\partial\overline{P}}{\partial\overline{R}}+\frac{1}{\overline{R}}\frac{\partial}{\partial\overline{R}}(\overline{R}\overline{\tau}_{rr})+\frac{\partial}{\partial\overline{Z}}\overline{\tau}_{rz}-\frac{\overline{\tau}_{\theta\theta}}{\overline{R}}+KN(\overline{U}_s-\overline{U}) \quad (5.9)$$

$$\rho\left[\overline{U}\frac{\partial\overline{W}}{\partial\overline{R}}+\overline{W}\frac{\partial\overline{W}}{\partial\overline{Z}}\right]=-\frac{\partial\overline{P}}{\partial\overline{Z}}+\frac{1}{\overline{R}}\frac{\partial}{\partial\overline{R}}\left(\overline{R}\overline{\tau}_{rz}\right)\frac{\partial}{\partial\overline{Z}}\overline{\tau}_{zz}+KN\left(\overline{W}_s-\overline{W}\right)-\rho g\alpha_1\left(\overline{T}-\overline{T}_0\right). \quad (5.10)$$

For solid particles

$$\overline{U}_s\frac{\partial\overline{U}_s}{\partial\overline{R}}+\overline{W}_s\frac{\partial\overline{U}_s}{\partial\overline{Z}}=\frac{K}{m}\left(\overline{U}-\overline{U}_s\right), \quad (5.11)$$

$$\overline{U}_s\frac{\partial\overline{W}_s}{\partial\overline{R}}+\overline{W}_s\frac{\partial\overline{W}_s}{\partial\overline{Z}}=\frac{K}{m}\left(\overline{W}-\overline{W}_s\right). \quad (5.12)$$

For energy equation

$$\rho C_p\left[\overline{U}\frac{\partial\overline{T}}{\partial\overline{R}}+\overline{W}\frac{\partial\overline{T}}{\partial\overline{Z}}\right]=\kappa\left[\frac{\partial^2\overline{T}}{\partial\overline{R}^2}+\frac{1}{\overline{R}}\frac{\partial\overline{T}}{\partial\overline{R}}+\frac{\partial\overline{T}^2}{\partial\overline{Z}^2}\right]+\overline{\tau}_{rr}\left(\frac{\partial\overline{U}}{\partial\overline{R}}\right)+\overline{\tau}_{zz}\left(\frac{\partial\overline{U}}{\partial\overline{Z}}\right)+\overline{\tau}_{rz}\left(\frac{\partial\overline{U}}{\partial\overline{R}}+\frac{\partial\overline{U}}{\partial\overline{Z}}\right). \quad (5.13)$$

Utilizing the provided transformations to establish a relationship between the mobile frame ($\overline{r}$,$\overline{z}$) and the stationary frames ($\overline{R}$,$\overline{Z}$).

$\overline{z} = \overline{Z} - c\overline{t}$, $\overline{r} = \overline{R}$, $\overline{w} = \overline{W} - c$, $\overline{u} = \overline{U}$, $\overline{w}_s = \overline{W}_s - c$, $\overline{u}_s = \overline{U}_s$.

Taking into consideration dimensionless parameters.

$$w=\frac{\overline{w}}{c},\ r=\frac{\overline{r}}{a},\ z=\frac{\overline{z}}{\lambda},\ p=\frac{a^2\overline{p}}{\lambda\mu c},\ \overline{u}_s=\frac{u_s}{\delta c},\ w_s=\frac{\overline{w}_s}{c},\ t=\frac{c\overline{t}}{\lambda},\ u=\frac{\overline{u}}{\delta c'},\ \delta=\frac{a}{\lambda},Re=\frac{\rho ca}{\mu},$$

$$\tau=\frac{a\,\overline{\tau}}{\mu c},\ \alpha_1=\frac{c\overline{\alpha_1}}{\mu a},\ A=\frac{KNa^2}{\mu},\ B=\frac{Ka}{mc},\ \phi=\frac{b}{a},\theta=\frac{\overline{T}-\overline{T}_0}{\Delta\overline{T}}.$$

Components of extra stress tensor are:

$$\tau_{rr}=2\delta\frac{\partial u}{\partial r}+\alpha_1\left[\left(\frac{\partial w}{\partial r}\right)^2+2\delta^2u\left(\frac{\partial^2u}{\partial r^2}\right)+2\delta^2w\left(\frac{\partial^2u}{\partial r\partial z}\right)-\delta^4\left(\frac{\partial u}{\partial z}\right)^2\right], \quad (5.14)$$

$$\tau_{rz}=\left(\delta^2\frac{\partial u}{\partial z}+\frac{\partial w}{\partial r}\right)+\alpha_1\left[\delta^3u\left(\frac{\partial^2u}{\partial r\partial z}\right)+\delta u\left(\frac{\partial^2\mathrm{w}}{\partial\mathrm{r}^2}\right)+\delta^3w\left(\frac{\partial^2u}{\partial z^2}\right)+\delta w\left(\frac{\partial^2w}{\partial r\partial z}\right)+\delta^3\left(\frac{\partial u}{\partial r}\right)\left(\frac{\partial u}{\partial z}\right)+\delta\left(\frac{\partial w}{\partial r}\right)\left(\frac{\partial w}{\partial z}\right)-\delta^3\left(\frac{\partial w}{\partial z}\right)\left(\frac{\partial u}{\partial z}\right)-\delta\left(\frac{\partial u}{\partial r}\right)\left(\frac{\partial w}{\partial r}\right)\right], \quad (5.15)$$

$$\tau_{zz}=2\,\delta\frac{\partial w}{\partial z}+\alpha_1\left[\delta^4\left(\frac{\partial u}{\partial z}\right)^2+2\delta^2u\left(\frac{\partial^2w}{\partial r\partial z}\right)+2\delta^2w\left(\frac{\partial^2w}{\partial z^2}\right)-\left(\frac{\partial w}{\partial r}\right)^2\right]. \quad (5.16)$$

The streamline conversions implied are:

$$u = -\frac{1}{r}\frac{\partial\psi}{\partial z} \quad , \quad w = \frac{1}{r}\frac{\partial\psi}{\partial r} \quad ,$$

$$u_s = -\frac{1}{r}\frac{\partial\phi}{\partial z} \quad , \quad w_s = \frac{1}{r}\frac{\partial\phi}{\partial r} \quad .$$

The compatibility equations for fluid and dust after removing the pressure gradient are:

$$Re\delta\left[\delta^2\left(\frac{-2}{r^2}\frac{\partial\psi}{\partial z}\frac{\partial^2\psi}{\partial z^2} + \frac{1}{r}\frac{\partial\psi}{\partial z}\frac{\partial^3\psi}{\partial r\partial z^2} - \frac{1}{r}\frac{\partial^3\psi}{\partial z^3}\frac{\partial\psi}{\partial r} - \frac{\partial^3\psi}{\partial z^3}\right)\right] = \delta\frac{\partial^2}{\partial r\partial z}(r\tau_{rr}) + \delta^2 r\frac{\partial^2\tau_{rz}}{\partial z^2} -$$
$$\delta\frac{\partial^2\tau_{\theta\theta}}{\partial z} - r\frac{\partial}{\partial r}\left(\frac{1}{r}\frac{\partial}{\partial r}\tau_{rz}\right) - \delta r\frac{\partial^2\tau_{zz}}{\partial r\partial z} - A\left(\nabla_1{}^2\varphi - \nabla_1{}^2\psi\right), \qquad (5.17)$$

$$\delta\left[\delta^2\left(\frac{-2}{r^2}\frac{\partial\varphi}{\partial z}\frac{\partial^2\varphi}{\partial z^2} + \frac{1}{r}\frac{\partial\varphi}{\partial z}\frac{\partial^3\varphi}{\partial r\partial z^2} - \frac{1}{r}\frac{\partial^3\varphi}{\partial z^3}\frac{\partial\varphi}{\partial r} - \frac{\partial^3\varphi}{\partial z^3}\right) - \left(-\frac{3}{r^3}\frac{\partial\varphi}{\partial r}\frac{\partial\varphi}{\partial z} + \frac{3}{r^2}\frac{\partial\varphi}{\partial z}\frac{\partial^2\varphi}{\partial r^2} - \frac{1}{r}\frac{\partial^3\varphi}{\partial r^3}\frac{\partial\varphi}{\partial z} -\right.\right.$$
$$\left.\left.\frac{1}{r^2}\frac{\partial\varphi}{\partial r}\frac{\partial^2\varphi}{\partial r\partial z} + \frac{1}{r}\frac{\partial\varphi}{\partial r}\frac{\partial^3\varphi}{\partial r^2\partial z} - \frac{1}{r}\frac{\partial^2\varphi}{\partial r\partial z} + \frac{\partial^3\varphi}{\partial r^2\partial z}\right)\right] = B(\nabla_1^2\varphi - \nabla_1^2\psi), \qquad (5.18)$$

$$\delta\, P_r\, Re\left[\left(-\frac{1}{r}\frac{\partial\psi}{\partial z}\right)\frac{\partial\theta}{\partial r} + \left(\frac{1}{r}\frac{\partial\psi}{\partial r}\right)\frac{\partial\theta}{\partial z}\right] = \left[\frac{1}{r}\frac{\partial\theta}{\partial r} + \frac{\partial^2\theta}{\partial r^2} + \delta^2\left(\frac{\partial^2\theta}{\partial z^2}\right)\right] +$$
$$Br\left[\delta\,\tau_{rr}\frac{\partial}{\partial r}\left(-\frac{1}{r}\frac{\partial\psi}{\partial z}\right) + \delta^2\,\tau_{zz}\frac{\partial}{\partial z}\left(-\frac{1}{r}\frac{\partial\psi}{\partial z}\right) + \tau_{rz}\left(\frac{\partial}{\partial r}\left(\frac{1}{r}\frac{\partial\psi}{\partial r}\right) +\right.\right.$$
$$\left.\left.\delta^2\frac{\partial}{\partial z}\left(-\frac{1}{r}\frac{\partial\psi}{\partial z}\right)\right)\right], \qquad (5.19)$$

where $\nabla_1^2 = \left(\delta^2\frac{\partial^2}{\partial z^2} + \frac{\partial^2}{\partial r^2} + \frac{1}{r}\frac{\partial}{\partial r}\right)$

We can formulate the boundary conditions in a dimensionless manner as follows:

$$\varphi = 0, \quad \psi = 0, \quad \frac{1}{r}\frac{\partial\psi}{\partial r} = -1, \quad \theta = 1\ at\ r = r_1 = \epsilon \ , \qquad (5.20)$$

$$\varphi = F, \quad \psi = F_s, \quad \frac{1}{r}\frac{\partial\psi}{\partial r} = -1, \quad \theta = 0\ at\ r = r_2 = 1 + \phi\sin 2\pi z \ . \qquad (5.21)$$

The fluid and solid granules exhibit dimensionless time flow as expressed by the following equations.

$$Q = F + \frac{1}{2}(1+\phi)^2 ,$$

$$Q_s = F_s + \frac{1}{2}(1+\phi)^2 ,$$

where

$$F = \int_0^h \frac{\partial\psi}{\partial r}dr = \psi(h) - \psi(0) , \qquad (5.22)$$

$$F_s = \int_0^h \frac{\partial\phi}{\partial r}dr = \phi(h) - \phi(0) . \qquad (5.23)$$

The formulation for the pressure rise is as follows:

$$\Delta p = \int_0^1 \frac{dp}{dz}dr$$

The equation (9) provides a representation of the $\frac{\mathrm{dp}}{\mathrm{dz}}$ in the following form:

$$\frac{dp}{dz} = \frac{1}{r}\frac{\partial}{\partial r}(rT_{rz}) + \delta\frac{\partial}{\partial z}(T_{zz}) + \frac{A}{r}\left(\frac{\partial\varphi}{\partial r} - \frac{\partial\psi}{\partial r}\right) - \delta Re\left[-\frac{1}{r}\frac{\partial\psi}{\partial z}\frac{\partial}{\partial r}\left(\frac{1}{r}\frac{\partial\psi}{\partial r}\right) + \left(\frac{1}{r}\frac{\partial\psi}{\partial r} + 1\right)\frac{\partial}{\partial z}\left(\frac{1}{r}\frac{\partial\psi}{\partial r}\right)\right]. \quad (5.24)$$

5.3 Solution Methodology

The equations governing the behavior of both the fluid and dust particles exhibit nonlinearity. To obtain a solution, a perturbation technique has been employed.

$$\psi = \psi_0 + \delta\psi_1 + \delta^2\psi_2 + O(\delta^3); \quad (5.25)$$

$$\varphi = \varphi_0 + \delta\varphi_1 + \delta^2\varphi_2 + O(\delta^3); \quad (5.26)$$

$$\theta = \theta_0 + \delta\theta_1 + \delta^2\theta_2 + O(\delta^3); \quad (5.27)$$

$$F = F_0 + \delta F_1 + \delta^2 F_2 + O(\delta^3); \quad (5.28)$$

$$F_s = F_{s0} + \delta F_{s1} + \delta^2 F_{s2} + O(\delta^3); \quad (5.29)$$

$$P = P_0 + \delta P_1 + \delta^2 P_2 + O(\delta^3); \quad (5.30)$$

5.3.1 Zeroth – Order System

$$-r\frac{\partial}{\partial r}\left[\frac{1}{r}\frac{\partial}{\partial r}(rT_{0rz})\right] - A\left[\frac{\partial^2}{\partial r^2} - \frac{1}{r}\frac{\partial}{\partial r}\right](\varphi_0 - \psi_0) = 0, \quad (5.31)$$

$$B\left[\frac{\partial^2}{\partial r^2} - \frac{1}{r}\frac{\partial}{\partial r}\right](\varphi_0 - \psi_0) = 0, \quad (5.32)$$

$$\left[\frac{\partial^2}{\partial r^2} - \frac{1}{r}\frac{\partial}{\partial r}\right]\theta_0 + Br\left[\tau_{0rz}\left(\frac{1}{r}\frac{\partial\psi_0}{\partial r}\right)\right] = 0, \quad (5.33)$$

$$\frac{dp_0}{dz} = \frac{1}{r}\frac{\partial}{\partial r}(rT_{0rz}) + \frac{A}{r}\left(\frac{\partial\varphi_0}{\partial r} - \frac{\partial\psi_0}{\partial x}\right), \quad (5.34)$$

where

$$T_{orz} = \frac{\partial w_0}{\partial r} = \frac{\partial}{\partial r}\left(\frac{1}{r}\frac{\partial\psi_0}{\partial r}\right).$$

With boundary conditions

$$\varphi_0 = 0, \quad \psi_0 = 0, \quad \frac{1}{r}\frac{\partial\psi_0}{\partial r} = -1, \quad \theta_0 = 1, \text{ at } r = r_1 = \epsilon, \quad (5.35)$$

$$\varphi_0 = F_{0s}, \quad \psi_0 = F_0, \quad \frac{1}{r}\frac{\partial\psi_0}{\partial r} = -1, \quad \theta_0 = 0, \text{ at } r = r_2 = 1 + \phi\sin 2\pi z. \quad (5.36)$$

5.3.2 First – Order System

$$Re[\frac{3}{r^3}\frac{\partial\psi_0}{\partial r}\frac{\partial\psi_0}{\partial z}-\frac{3}{r^2}\frac{\partial\psi_0}{\partial z}\frac{\partial^2\psi_0}{\partial r^2}+\frac{1}{r}\frac{\partial\psi_0}{\partial z}\frac{\partial^3\psi_0}{\partial r^3}+\frac{1}{r}\frac{\partial\psi_0}{\partial r}\frac{\partial^2\psi_0}{\partial r\partial z}-\frac{1}{r}\frac{\partial\psi_0}{\partial z}\frac{\partial^3\psi_0}{\partial r^2\partial z}+\frac{1}{r}\frac{\partial^2\psi_0}{\partial r\partial z}-\frac{\partial^3\psi_0}{\partial r^2\partial z}]=$$
$$\frac{\partial^2}{\partial r\partial z}(rT_{0rr})-r\frac{\partial}{\partial r}[\frac{1}{r}\frac{\partial}{\partial r}(rT_{1rz})]-r\frac{\partial^2}{\partial r\partial z}T_{0zz}-A(-\frac{1}{r}\frac{\partial}{\partial r}+\frac{\partial^2}{\partial r^2})(\varphi_1-\psi_1)\,, \qquad (5.37)$$

$$\frac{3}{r^3}\frac{\partial\varphi_0}{\partial r}\frac{\partial\varphi_0}{\partial z}-\frac{3}{r^2}\frac{\partial\varphi_0}{\partial z}\frac{\partial^2\varphi_0}{\partial r^2}+\frac{1}{r}\frac{\partial\varphi_0}{\partial z}\frac{\partial^3\varphi_0}{\partial r^3}+\frac{1}{r}\frac{\partial\varphi_0}{\partial r}\frac{\partial^2\varphi_0}{\partial r\partial z}-\frac{1}{r}\frac{\partial\varphi_0}{\partial z}\frac{\partial^3\varphi_0}{\partial r^2\partial z}+\frac{1}{r}\frac{\partial^2\varphi_0}{\partial r\partial z}$$
$$-\frac{\partial^3\varphi_0}{\partial r^2\partial z}=B\left(-\frac{1}{r}\frac{\partial}{\partial r}+\frac{\partial^2}{\partial r^2}\right)(\varphi_1-\psi_1)\,, \qquad (5.38)$$

$$\left(\frac{\partial^2}{\partial r^2}-\frac{1}{r}\frac{\partial}{\partial r}\right)\theta_1+Br\left[\tau_{0rr}\frac{\partial}{\partial r}\left(-\frac{1}{r}\frac{\partial\psi_0}{\partial z}\right)+\tau_{1rz}\frac{\partial}{\partial r}\left(\frac{1}{r}\frac{\partial\psi_0}{\partial r}\right)\right]=RePr\left[-\frac{1}{r}\frac{\partial\psi_0}{\partial z}\frac{\partial\theta_0}{\partial r}+\right.$$
$$\left.\left(\frac{1}{r}\frac{\partial\psi_0}{\partial r}+1\right)\frac{\partial\theta_0}{\partial z}\right], \qquad (5.39)$$

$$\frac{dp_1}{dz}=\frac{1}{r}\frac{\partial}{\partial r}(rT_{1rz})+\frac{\partial}{\partial z}(T_{0ZZ})+\frac{A}{r}\left(\frac{\partial\varphi_1}{\partial r}-\frac{\partial\psi_1}{\partial r}\right)-Re[-\frac{1}{r}\frac{\partial\psi_0}{\partial z}\frac{\partial}{\partial r}\left(\frac{1}{r}\frac{\partial\psi_0}{\partial r}\right)+\left(\frac{1}{r}\frac{\partial\psi_0}{\partial r}+\right.$$
$$\left.1\right)\frac{\partial}{\partial z}\left(\frac{1}{r}\frac{\partial\psi_0}{\partial r}\right)]\,, \qquad (5.40)$$

where

$$T_{0rr}=\alpha_1(\frac{\partial}{\partial r}\left(\frac{1}{r}\frac{\partial\psi_0}{\partial r}\right))^2, \qquad (5.41)$$

$$T_{1rz}=\frac{\partial}{\partial r}\left(\frac{1}{r}\frac{\partial\psi_1}{\partial r}\right)-\frac{1}{r}\frac{\partial^2}{\partial z^2}+\alpha_1\left[\frac{\partial}{\partial r}\left(\frac{1}{r}\frac{\partial\psi_0}{\partial r}\right)\frac{1}{r}\frac{\partial^2\psi_0}{\partial r\partial z}+\frac{\partial}{\partial r}\left(\frac{1}{r}\frac{\partial\psi_0}{\partial r}\right)\frac{1}{r}\frac{\partial^2\psi_0}{\partial r\partial z}-\frac{1}{r}\frac{\partial\psi_0}{\partial z}\frac{\partial^2}{\partial r^2}\left(\frac{1}{r}\frac{\partial\psi_0}{\partial r}\right)+\right.$$
$$\left.\frac{1}{r}\frac{\partial\psi_0}{\partial r}\frac{\partial^2}{\partial r\partial z}\left(\frac{1}{r}\frac{\partial\psi_0}{\partial r}\right)\right], \qquad (5.42)$$

$$T_{0zz}=-\alpha_1\left(\frac{\partial}{\partial r}\left(\frac{1}{r}\frac{\partial\psi_1}{\partial r}\right)\right), \qquad (5.43)$$

with boundary conditions

$$\varphi_1=0,\qquad \psi_1=0,\qquad \frac{\partial}{\partial r}\left(\frac{1}{r}\frac{\partial\psi_1}{\partial r}\right)=0,\qquad \frac{\partial\theta_1}{\partial r}=0\ \text{, at}\ \ r=r_1=\epsilon\,, \qquad (5.44)$$

$$\varphi_1=F_{s1},\quad \psi_1=F_1,\qquad \frac{1}{r}\frac{\partial\psi_1}{\partial r}=0,\qquad \theta_1=0\ \text{, at}\ \ r=r_2=1+\phi\sin 2\pi z\ . \qquad (5.45)$$

Graphs

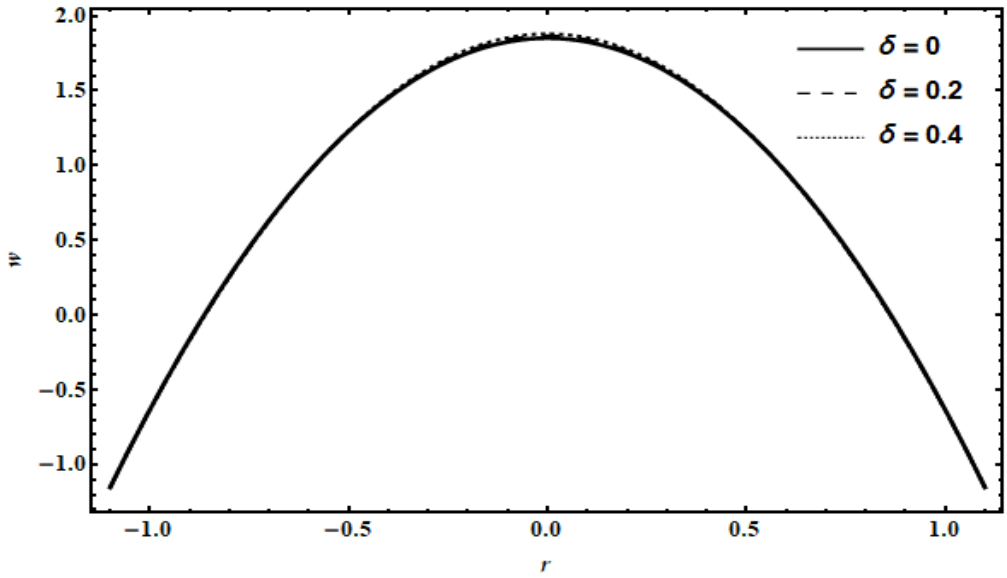

Figure 5.2: Influence of the wave number δ on fluid's velocity.

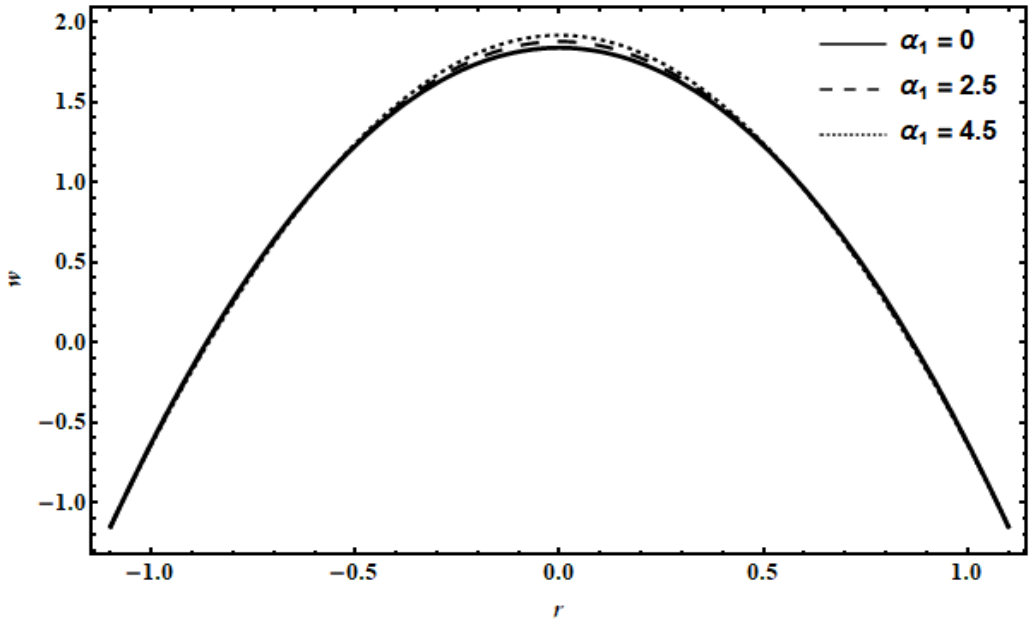

Figure 5.3: Influence of the second-grade parameter α_1 on fluid's velocity.

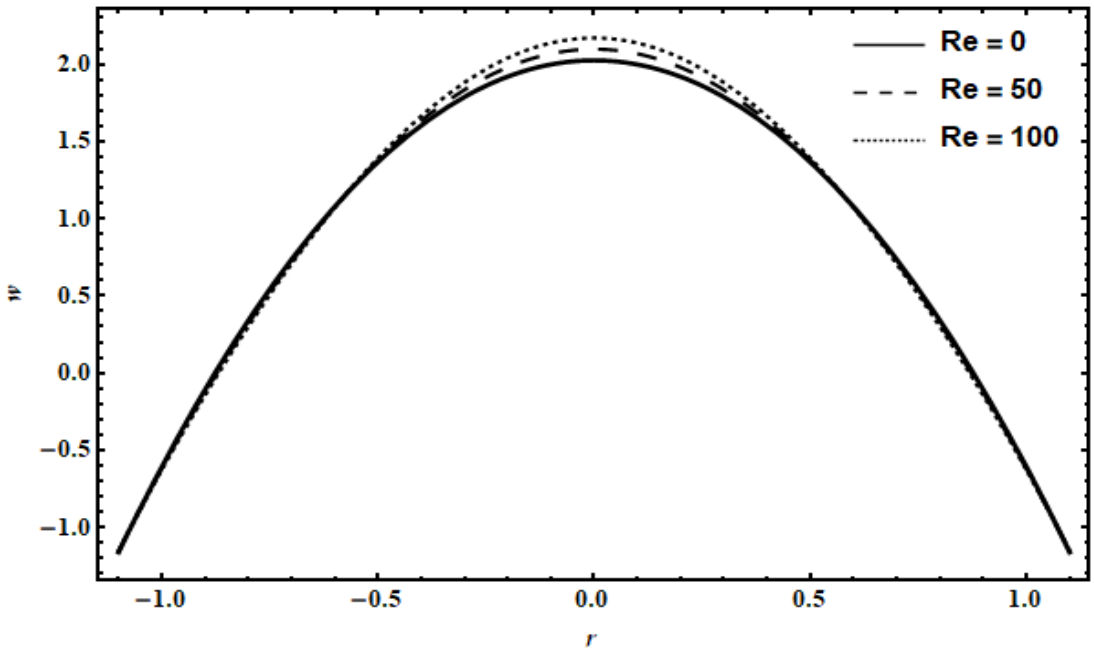

Figure 5.4: Influence of the Reynolds number Re on fluid's velocity.

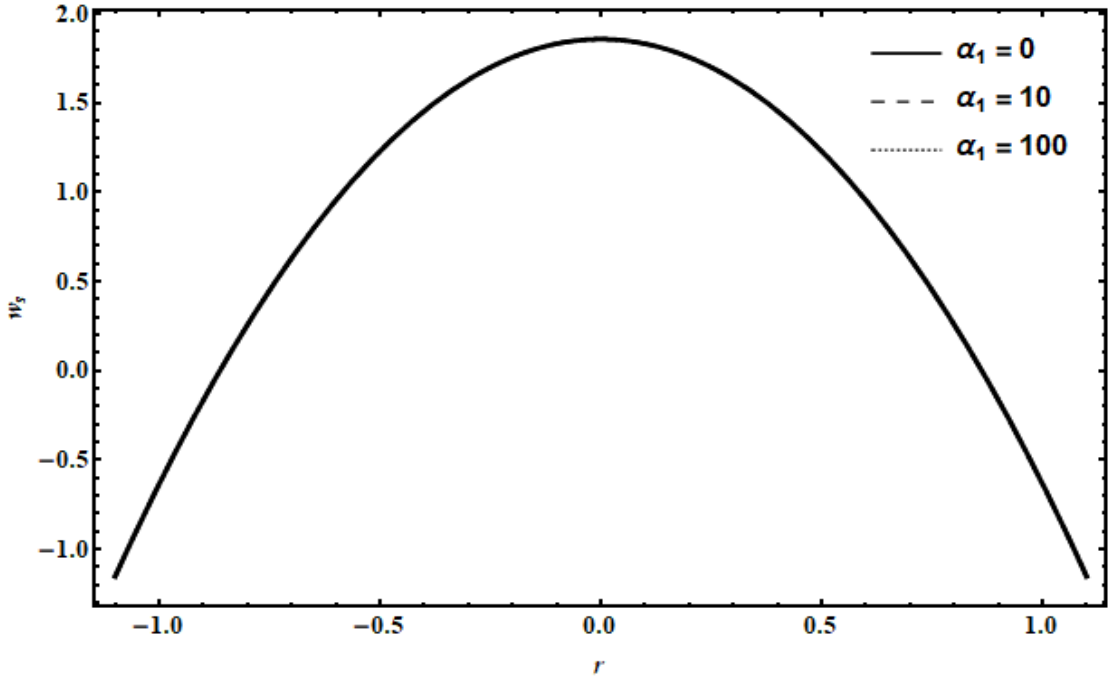

Figure 5.5: Influence of the second-grade parameter α_1 on Solid Particle's velocity.

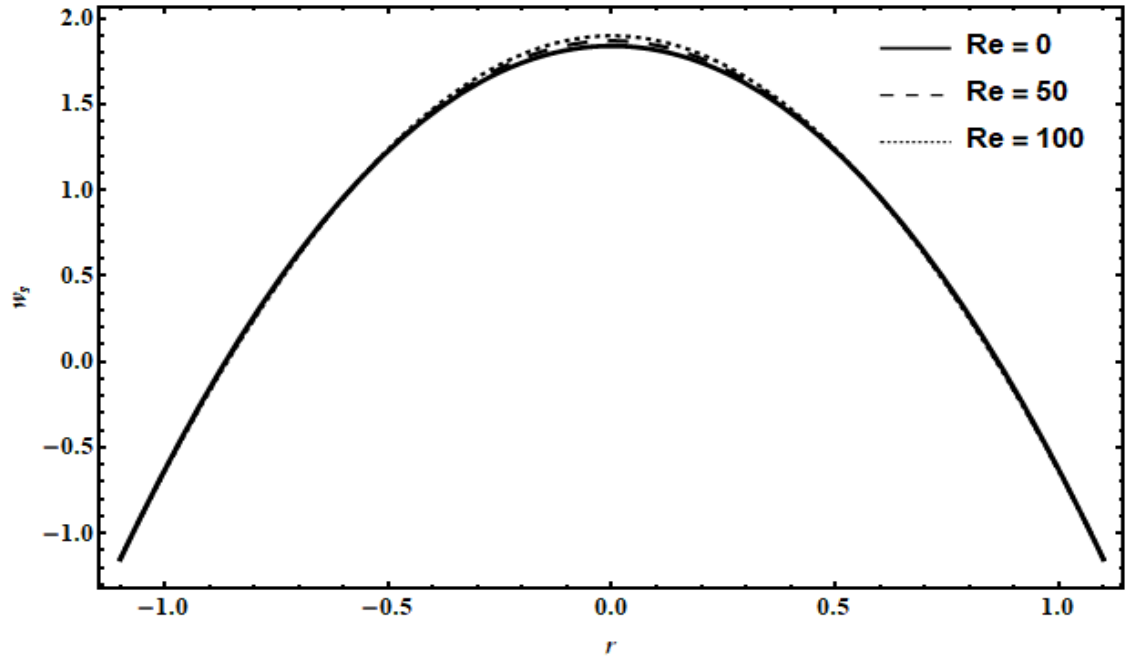

Figure 5.6: Influence of the Reynolds number Re on solid particle's velocity.

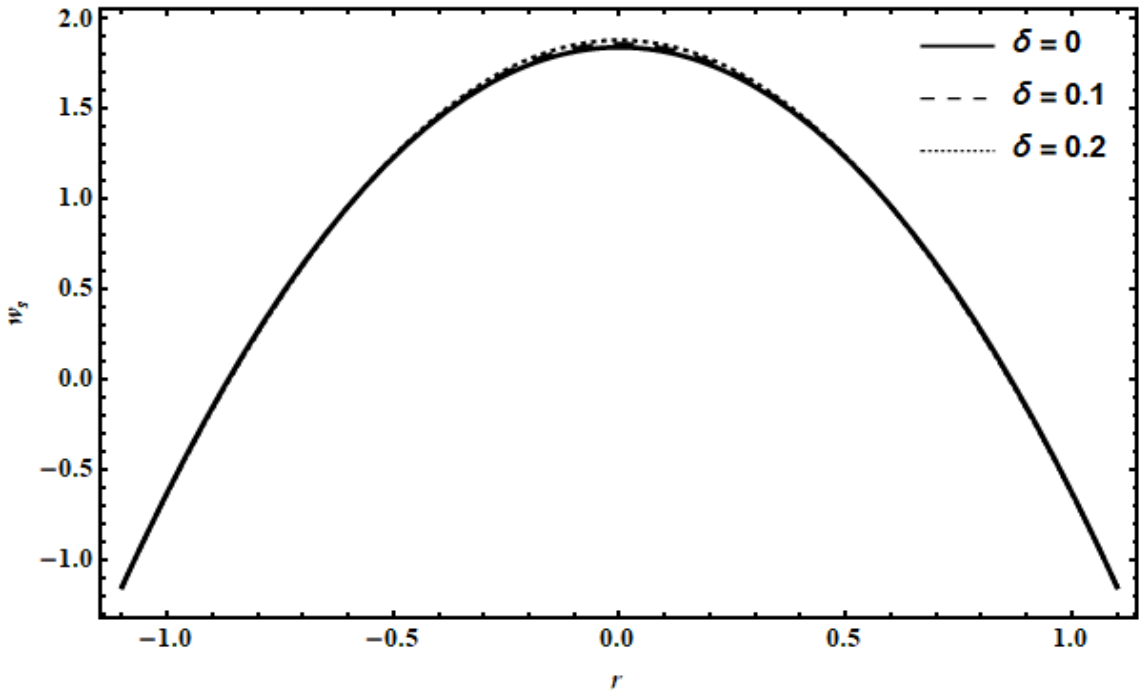

Figure 5.7: Influence of the wave number δ on solid particle's velocity

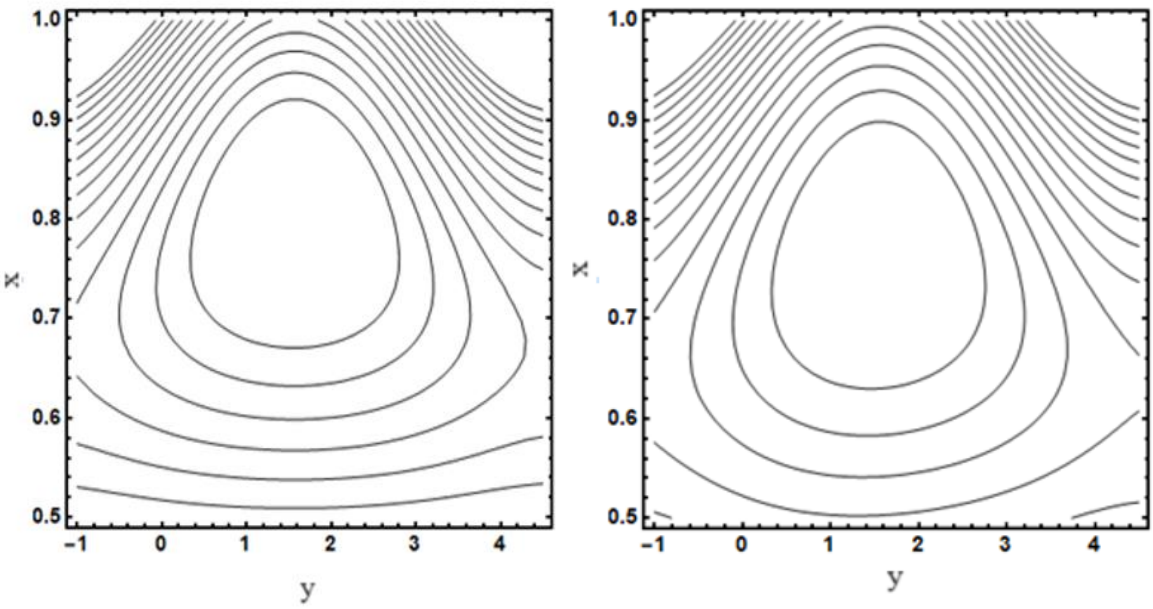

$(a)\ \alpha_1 = 0$ $(b)\ \alpha_1 = 5$

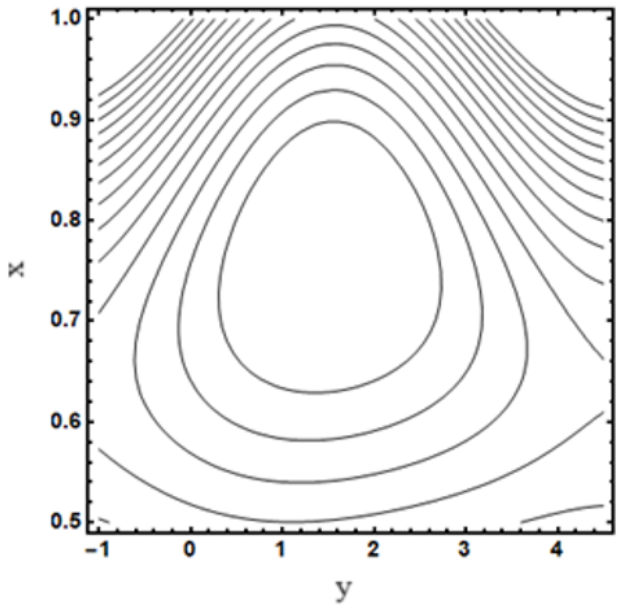

$(c)\ \alpha_1 = 10$

Figure 5.8: Streamline patterns of the fluid showing the impact of second-grade parameterα_1.

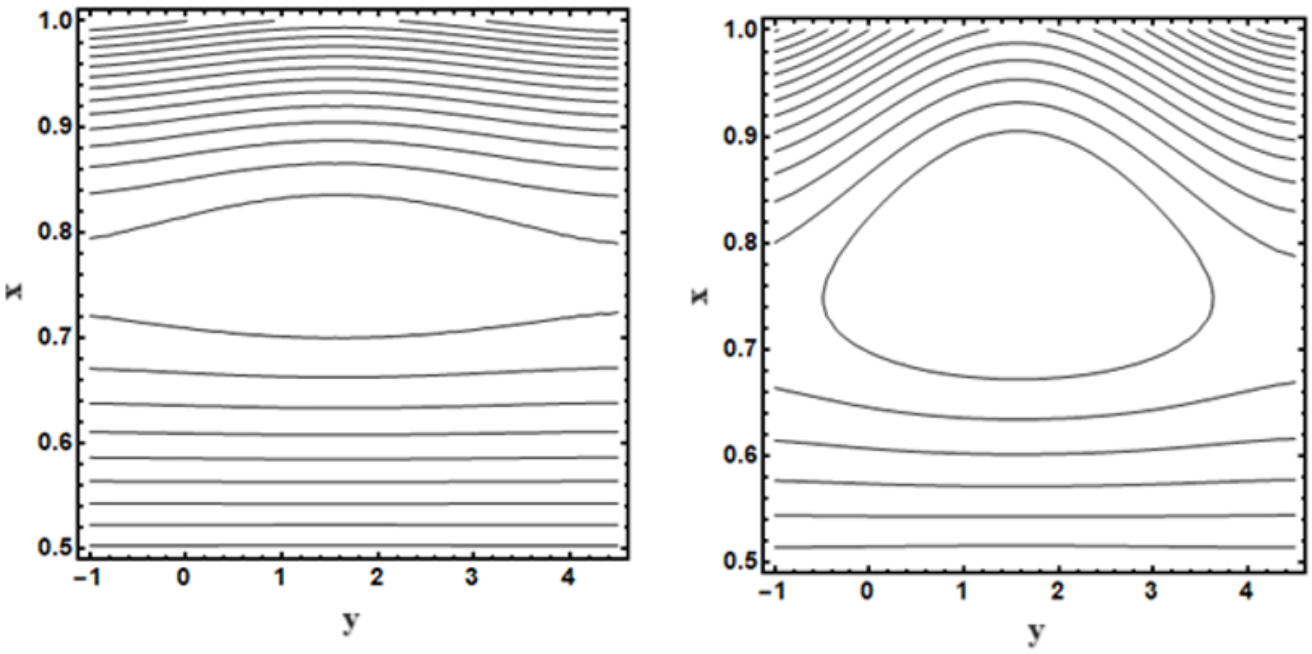

$(a)\ \epsilon = 0$ $(b)\ \epsilon = 0.05$

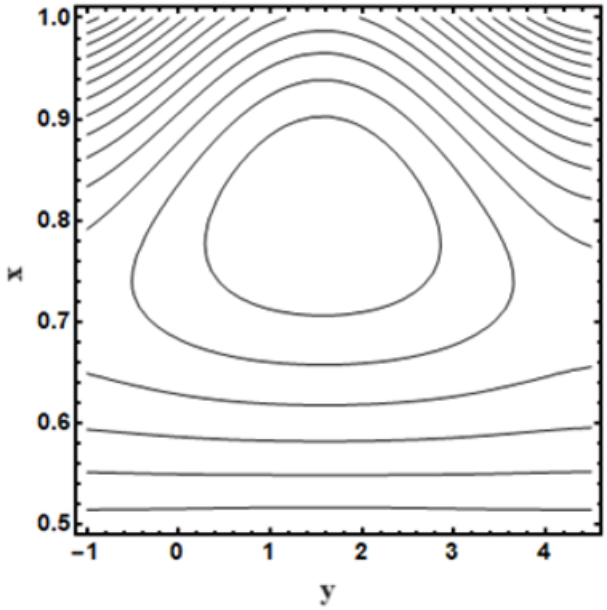

$(c)\ \epsilon = 0.1$

Figure 5.9: Streamline patterns of the fluid showing the impact of ϵ.

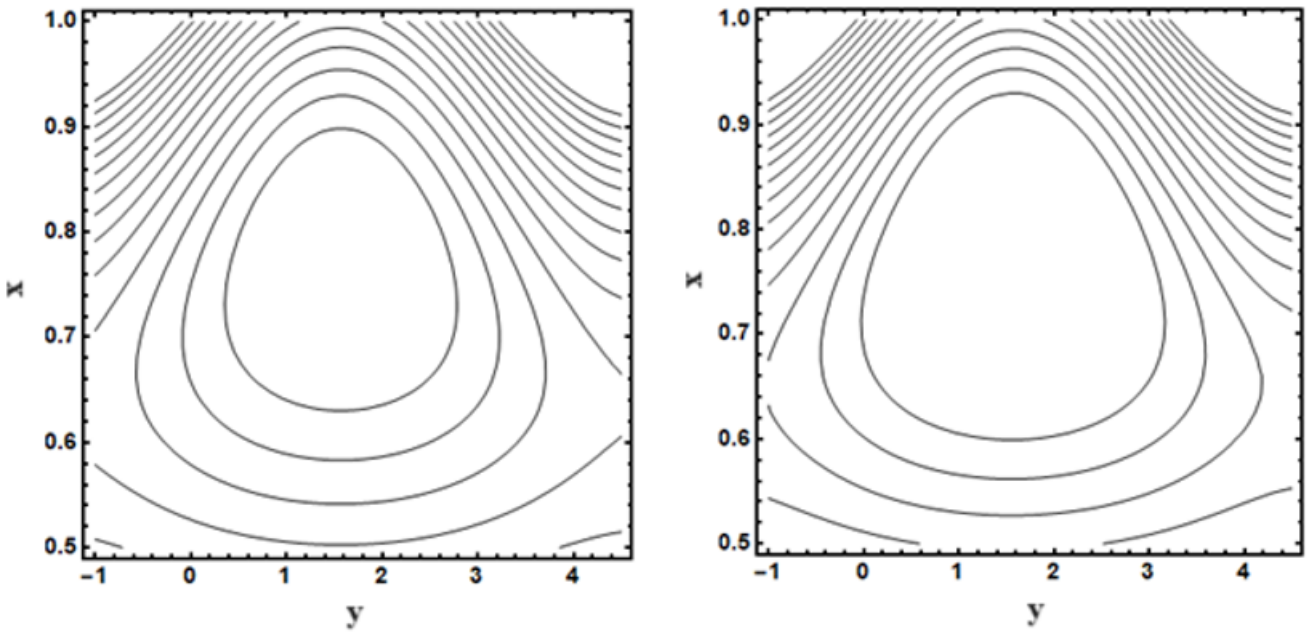

$Re = 0$ $Re = 50$

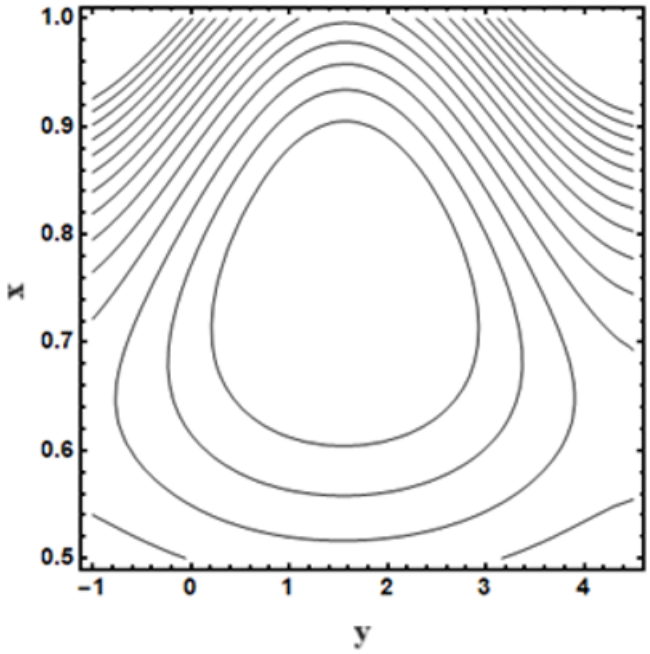

$Re = 100$

Figure 5.10: Streamline patterns of the fluid showing the impact of Re.

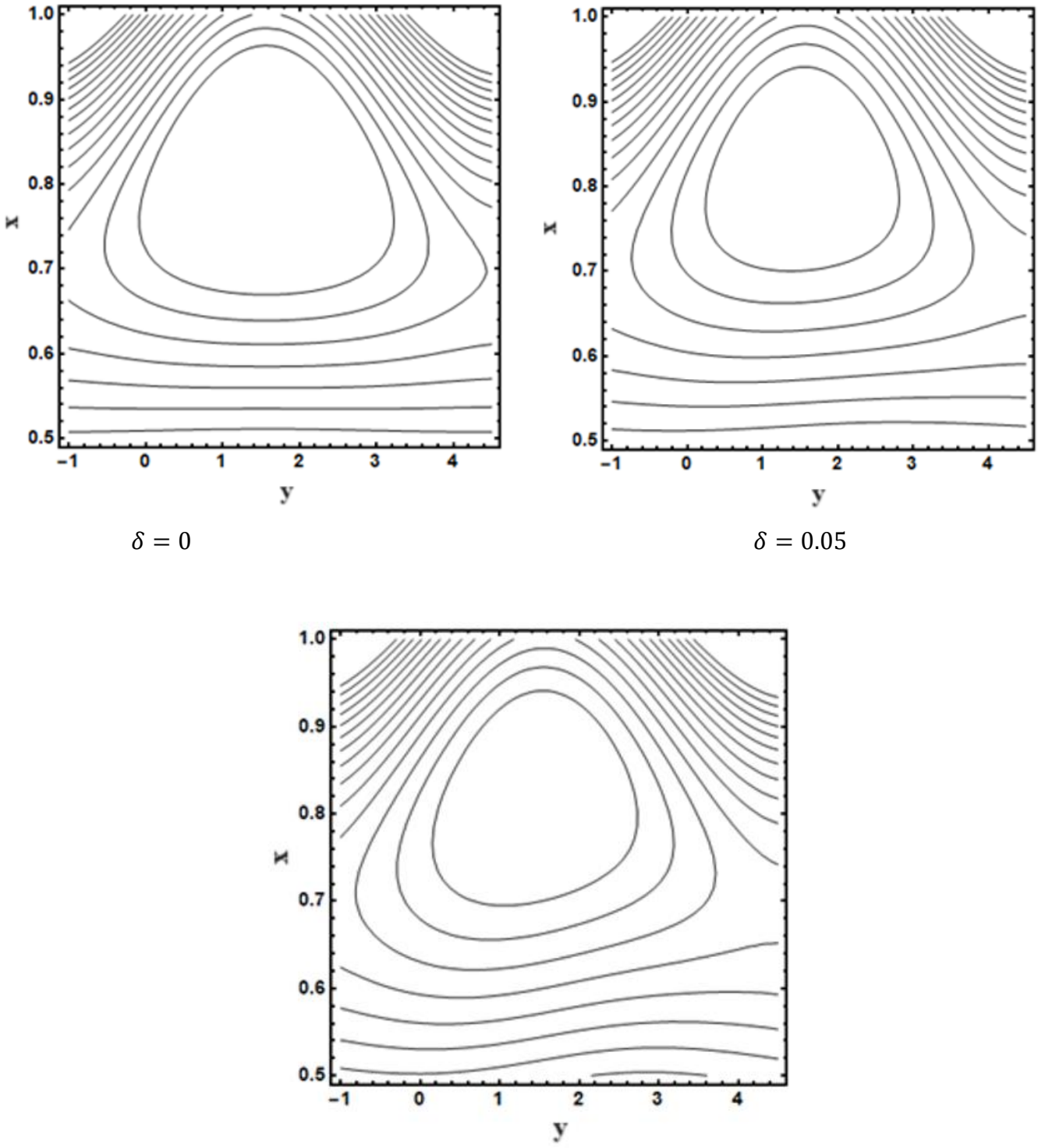

$\delta = 0$ $\delta = 0.05$

$\delta = 0.08$

Figure 5.11: Streamline patterns of the solid particles showing the impact of δ.

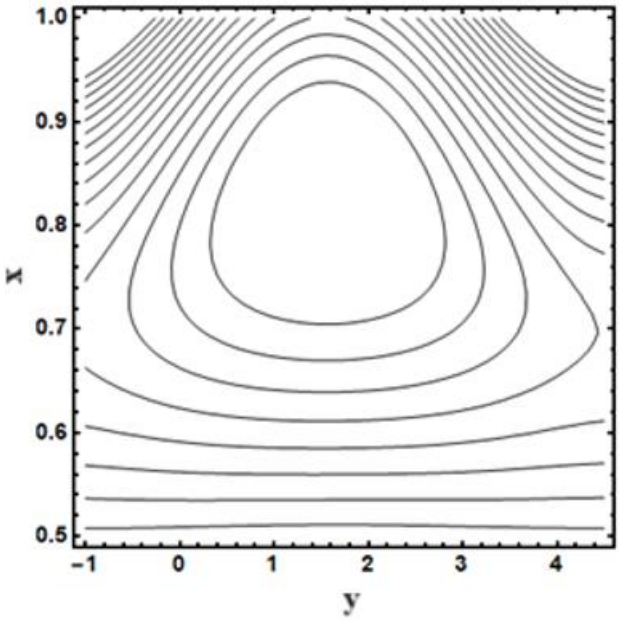

$Re = 0$

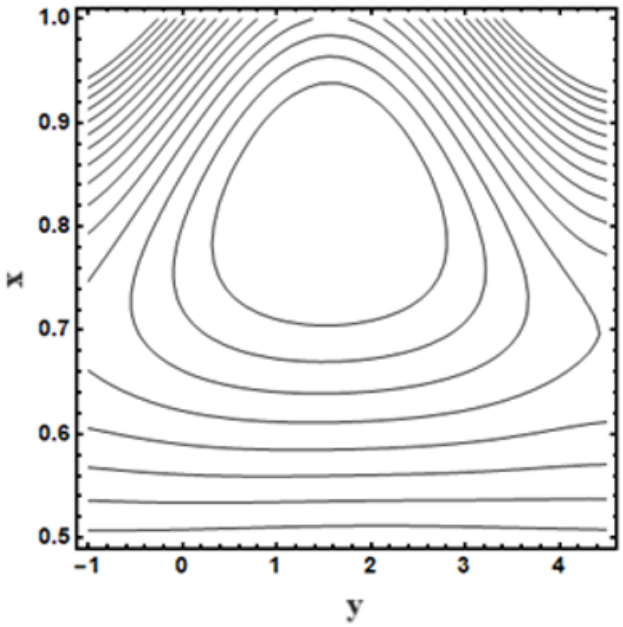

$Re = 50$

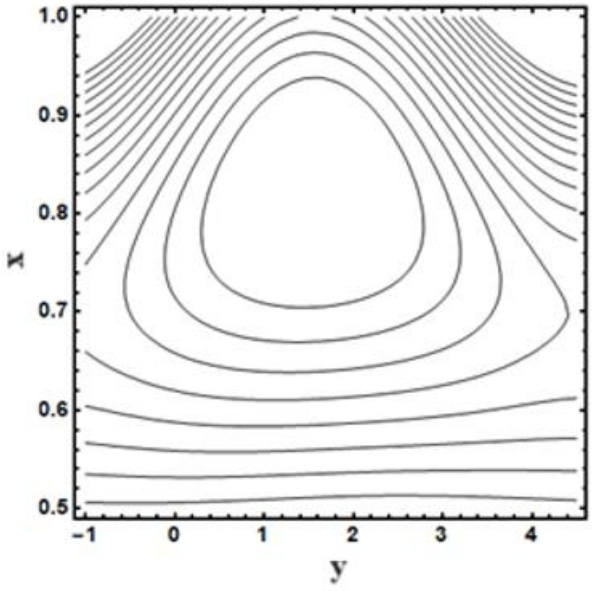

$Re = 150$

Figure 5.12: Streamline patterns of the solid particles showing the impact of *Re*.

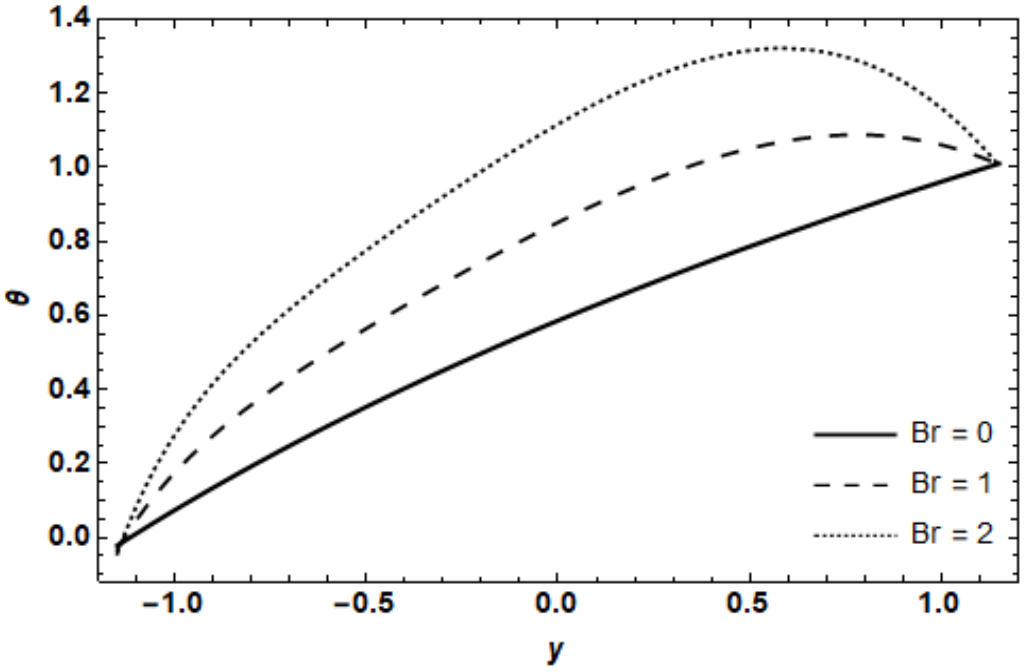

Figure 5.13: Temperature Profile of the fluid for the Brickman number (Br).

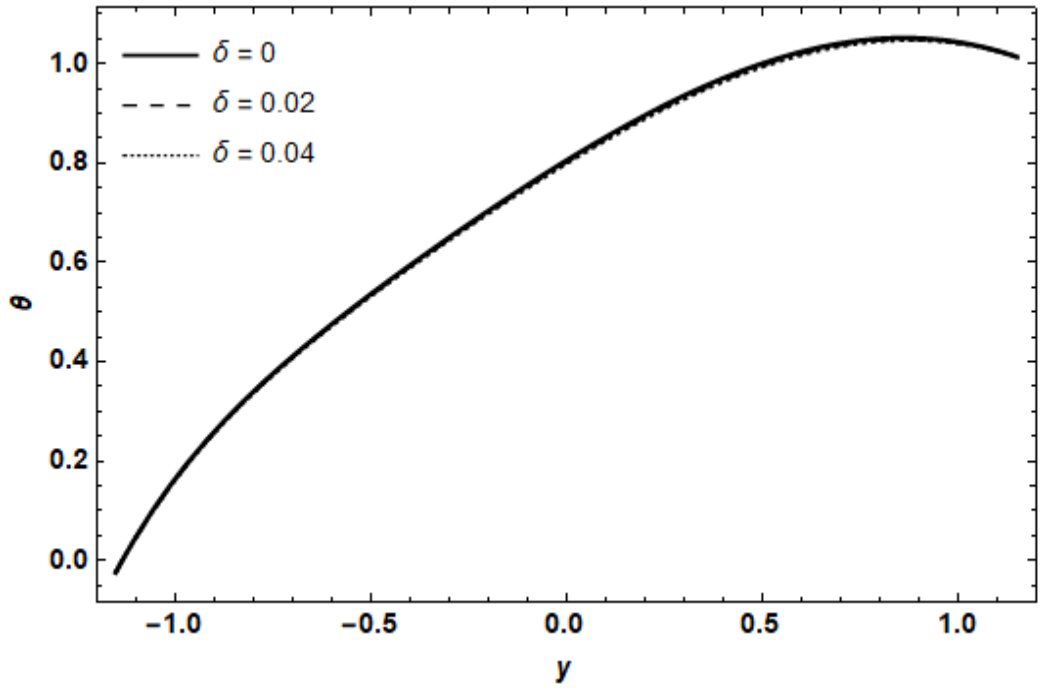

Figure 5.14: Temperature Profile of the fluid for the wave number (δ).

5.4 Results and Discussion

In this section, our primary focus is on investigating the impact of various parameters on velocity, streamline patterns, and pressure elevation. Figures 5.2 to 5.4 illustrate the influence on fluid velocity attributed to the Reynolds number (Re), a secondary characteristic denoted by α_1, and the wave number represented by δ.

Figures 5.5 to 5.7 delve into the relationship between the velocity of solid grains and parameters such as $\alpha_1, Re,$ and δ. It is observed that the velocity increases concerning both δ and Reynolds number, indicating enhanced movement of solid grains. The increase in Reynolds number signifies a decrease in viscous forces, facilitating a smoother flow of particles.

However, the influence of the second-grade parameter α_1 on velocity differs. Figure 5.8 demonstrates its impact on the fluid's stream pattern, showcasing a decrease in viscosity with increasing shear rates. Figure 5.9 displays the streamline pattern under the influence of ϵ.

In Figure 5.10, the influence of Reynolds number Re on the streamline pattern is depicted. As the Reynolds number increases, a weakening of viscous forces is observed, resulting in a more fluid motion. This causes the bolus to expand and move upward.

Figure 5.11 highlights how the contour patterns of solid grains are influenced by δ. An evident expansion in the bolus's volume is noted as the wave number increases, indicating an expanding movement of particles. Figure 5.12 illustrates that the rise in Reynolds number Re leads to the enlargement of the bolus, visually emphasizing the impact.

Moving to temperature distribution, Figure 5.13 plots θ versus y for various values of Br (Brinkman number). The temperature increases as the Brinkman number increases. Similarly, in Figure 5.14, the temperature profile increases with the wave number δ. Particularly, the shape of the temperature profile in both figures is almost parabolic.

Physically interpreting these observations, the increase in Reynolds number indicates a reduction in viscous forces, promoting smoother particle motion. The decrease in viscosity with increasing shear rates, as shown in Figure 5.8, suggests a more streamlined flow. The parabolic shape in temperature profiles (Figures 5.13 and 5.14) may indicate a balance between heat generation and dissipation in the system.

CHAPTER 6

CONCLUSION

This research investigates the peristaltic flow of a second-grade dusty fluid within an endoscope, incorporating the modeling of fine dust particles and fluid motion through the cylindrical tube with nonlinear coupled differential equations and which were analytically solved using a perturbation technique. The solutions for the modeled equations were computed using DSolver in Mathematica software. Key conclusions drawn from the study include:

The velocity of both dust grains and the fluid experiences an increase with variations in the parameter δ and Reynolds number Re. The bolus expands as the wave number increases for both fluid and dust particles. As the Reynolds number Re values increased, there was observable enlargement in the trapped bolus of both fluid and solid particles. The fluid velocity rises with increasing values of the second-grade parameter α_1, while no alteration in the velocity of solid granules was noted up to at least (δ^2). As the radius ratio ϵ increases, the bolus stretches upward within the channel.The increase in Brickman (Br) values associated with a rise in the temperature of the suspended particle fluid.

These findings significantly contribute to the understanding of peristaltic flow in complex systems and hold relevance for applications in medical endoscopy and fluid dynamics.

Future Work

We can extend this research by exploring various fluid models in the context of an endoscope. Additionally, we have considered different geometries for the endoscope, moving forward, we could examine other geometries to broaden the scope of our study such as planar channel, curved channel, symmetric channel etc. Furthermore, our current focus involves the second-grade parameter along with viscous dissipation. To extend this, we can explore different parameters, like considering the endoscope as porous or applying a magnetic field. These extensions will provide a more comprehensive understanding of peristaltic flow in diverse scenarios.

References

[1] Elshehawey, E. F., Eldabe, N. T., Elghazy, E. M., & Ebaid, A. (2006). Peristaltic transport in an asymmetric channel through a porous medium. Applied Mathematics and computation, 182(1), 140-150.

[2] Elmaboud, Y. A., Mekheimer, K. S., & Emam, T. G. (2019). Numerical examination of gold nanoparticles as a drug carrier on peristaltic blood flow through physiological vessels: cancer therapy treatment. BioNanoScience, 9, 952-965.

[3] Yadav, A., Bhushan, S., & Tripathi, D. (2018). Peristaltic pumping through porous medium in presence of electric double layer. In MATEC Web of Conferences (Vol. 192, p. 02043). EDP Sciences.

[4] Rundora, L., & Makinde, O. D. (2018). Unsteady MHD flow of non-newtonian fluid in a channel filled with a saturated porous medium with asymmetric navier slip and convective heating.

[5] Hina, S., & Yasin, M. (2018). Slip effects on peristaltic flow of magneto hydrodynamics second grade fluid through a flexible channel with heat/mass transfer. Journal of Thermal Science and Engineering Applications, 10(5).

[6] Tripathi, D. (2011). Peristaltic flow of a fractional second grade fluid through a cylindrical tube. Thermal Science, 15(suppl. 2), 167-173.

[7] Vaidya, H., Makinde, O. D., Choudhari, R., Prasad, K. V., Khan, S. U., & Vajravelu, K. (2020). Peristaltic flow of non-Newtonian fluid through an inclined complaint nonlinear tube: application to chyme transport in the gastrointestinal tract. The European Physical Journal Plus, 135(11), 1-15.

[8] Prakash, J., Ansu, A. K., & Tripathi, D. (2018). Alterations in peristaltic pumping of Jeffery Nano liquids with electric and magnetic fields. Meccanica, 53, 3719-3738.

[9] Bhatti, M. M., Zeeshan, A., Ellahi, R., Bég, O. A., & Kadir, A. (2019). Effects of coagulation on the two-phase peristaltic pumping of magnetized Prandtl biofluid through an endoscopic annular geometry containing a porous medium. Chinese Journal of Physics, 58, 222-234.

[10] Ma, T., Sun, S., Li, B., & Chu, J. (2019). Piezoelectric peristaltic micro pump integrated on a microfluidic chip. Sensors and Actuators A: Physical, 292, 90-96.

[11] Butt, A. W., Akbar, N. S., & Mir, N. A. (2020). Heat transfer analysis of peristaltic flow of a Phan-Thien–Tanner fluid model due to metachronal wave of cilia. Biomechanics and modeling in mechanobiology, 19, 1925-1933.

[12] Haque, E. U., Awan, A. U., Raza, N., Abdullah, M., & Chaudhry, M. A. (2018). A computational approach for the unsteady flow of Maxwell fluid with Caputo fractional derivatives. Alexandria engineering journal, 57(4), 2601-2608.

[13] Rafiq, M., Sajid, M., Alhazmi, S. E., Khan, M. I., & El-Zahar, E. R. (2022). MHD electroosmotic peristaltic flow of Jeffrey nanofluid with slip conditions and chemical reaction. Alexandria Engineering Journal, 61(12), 9977-9992.

[14] Esser, F., Masselter, T., & Speck, T. (2019). Silent pumpers: a comparative topical overview of the peristaltic pumping principle in living nature, engineering, and biomimetics. Advanced Intelligent Systems, 1(2), 1900009.

[15] Asha, S. K., & Sunitha, G. (2020). Thermal radiation and Hall effects on peristaltic blood flow with double diffusion in the presence of nanoparticles. Case Studies in Thermal Engineering, 17, 100560.

[16] Vaidya, H., Rajashekhar, C., Prasad, K. V., Khan, S. U., Mebarek-Oudina, F., Patil, A., & Nagathan, P. (2021). Channel flow of MHD Bingham fluid due to peristalsis with multiple chemical reactions: an application to blood flow through narrow arteries. SN Applied Sciences, 3, 1-12.

[17] Forouzandeh, F., Arevalo, A., Alfadhel, A., & Borkholder, D. A. (2021). A review of peristaltic micro pumps. Sensors and Actuators A: Physical, 326, 112602.

[18] Hussain, F., Ellahi, R., Zeeshan, A., & Vafai, K. (2018). Modelling study on heated couple stress fluid peristaltically conveying gold nanoparticles through coaxial tubes: a remedy for gland tumors and arthritis. Journal of Molecular Liquids, 268, 149-155.

[19] Nadeem, S., Akhtar, S., & Saleem, A. (2021). Peristaltic flow of a heated Jeffrey fluid inside an elliptic duct: streamline analysis. Applied Mathematics and Mechanics, 42, 583-592.

[20] Abd-Alla, A. M., Thabet, E. N., & Bayones, F. S. (2022). Numerical solution for MHD peristaltic transport in an inclined nanofluid symmetric channel with porous medium. Scientific Reports, 12(1), 3348.

[21] Saffman, P. G. (1962). On the stability of laminar flow of a dusty gas. Journal of fluid mechanics, 13(1), 120-128.

[22] Manjunatha, P. T., Gireesha, B. J., & Prasannakumara, B. C. (2014). Thermal analysis of conducting dusty fluid flow in a porous medium over a stretching cylinder in the presence of non-uniform source/sink. International journal of mechanical and materials engineering, 9, 1-10.

[23] Siddiqa, S., Hossain, M. A., & Saha, S. C. (2015). Two-phase natural convection flow of a dusty fluid. International Journal of Numerical Methods for Heat & Fluid Flow, 25(7), 1542-1556.

[24] Prasannakumara, B. C., Gireesha, B. J., & Manjunatha, P. T. (2015). Melting phenomenon in MHD stagnation point flow of dusty fluid over a stretching sheet in the presence of thermal radiation and non-uniform heat source/sink. International Journal for Computational Methods in Engineering Science and Mechanics, 16(5), 265-274.

[25] Turkyilmazoglu, M. (2017). Magnetohydrodynamic two-phase dusty fluid flow and heat model over deforming isothermal surfaces. Physics of Fluids, 29(1), 013302.

[26] Siddiqa, S., Begum, N., Hossain, M. A., Shoaib, M., & Reddy Gorla, R. S. (2018). Radiative heat transfer analysis of non-Newtonian dusty Casson fluid flow along a complex wavy surface. Numerical Heat Transfer, Part A: Applications, 73(4), 209-221.

[27] Bilal, M., Khan, S., Ali, F., Arif, M., Khan, I., & Nisar, K. S. (2021). Couette flow of viscoelastic dusty fluid in a rotating frame along with the heat transfer. Scientific reports, 11(1), 506.

[28] Khan, A. A., & Tariq, H. (2020). Peristaltic flow of second-grade dusty fluid through a porous medium in an asymmetric channel. Journal of Porous Media, 23(9).

[29] Khan, Z., ul Haq, S., Ali, F., & Andualem, M. (2022). Free convection flow of second grade dusty fluid between two parallel plates using Fick's and Fourier's laws: a fractional model. Scientific Reports, 12(1), 3448.

[30] Khan, Z., Ali, F., Haq, S. U., & Khan, I. (2022). A time fractional second-grade magnetohydrodynamic dusty fluid flow model with variable conditions: Application of Fick's and Fourier's laws. Frontiers in Physics, 983.

[31] Khan, A. A., & Tariq, H. (2018). Influence of wall properties on the peristaltic flow of a dusty Walter's B fluid. Journal of the Brazilian Society of Mechanical Sciences and Engineering, 40(8), 368.

[32] Tariq, H., & Khan, A. A. (2020). Peristaltic transport of a second-grade dusty fluid in a tube. J. Mech. Eng. Res, 11(2), 11-25.

[33] Mishra, S. R., Sun, T. C., Rout, B. C., Khan, M. I., Alaoui, M. K., & Khan, S. U. (2022). Control of dusty Nano fluid due to the interaction on dust particles in a conducting medium: Numerical investigation. Alexandria Engineering Journal, 61(4), 3341-3349.

[34] Ahmed, S. E., & Rashed, Z. Z. (2021). Magnetohydrodinamic dusty hybrid nanofluid peristaltic flow in curved channels. Thermal Science, 25(6 Part A), 4241-4255.

[35] Ali, K., Ahmad, S., Aamir, M., Jamshed, W., Pasha, A. A., & Hussain, S. M. (2022). Application of the successive over relaxation method for analyzing the dusty flow over a surface subject to convective boundary condition. Ain Shams Engineering Journal, 102044.
[36] Rashed, Z. Z., & Ahmed, S. E. (2021). Peristaltic flow of dusty nanofluids in curved channels. Compute. Mater. Continua, 66(1), 1012-1026.
[37] Khan, A. A. (2021). Peristaltic movement of a dusty fluid in a curved configuration with mass transfer. Punjab University Journal of Mathematics, 53(1).
[38] Turkyilmazoglu, M. (2018). Analytical solutions to mixed convection MHD fluid flow induced by a nonlinearly deforming permeable surface. Communications in Nonlinear Science and Numerical Simulation, 63, 373-379.
[39] Xu, C., Nie, W., Liu, Z., Peng, H., Yang, S., & Liu, Q. (2019). Multi-factor numerical simulation study on spray dust suppression device in coal mining process. Energy, 182, 544-558.
[40] Xiu, Z., Nie, W., Yan, J., Chen, D., CAI, P., Liu, Q., & Yang, B. (2020). Numerical simulation study on dust pollution characteristics and optimal dust control air flow rates during coal mine production. Journal of Cleaner Production, 248, 119197.
[41] Ghadikolaei, S. S., Hosseinzadeh, K., Hatami, M., & Ganji, D. D. (2018). MHD boundary layer analysis for micropolar dusty fluid containing Hybrid nanoparticles (Cu-Al2O3) over a porous medium. Journal of Molecular Liquids, 268, 813-823.
[42] Turkyilmazoglu, M. (2020). Suspension of dust particles over a stretchable rotating disk and two-phase heat transfer. International Journal of Multiphase Flow, 127, 103260.
[43] Afridi, M. I., Ashraf, M. U., Qasim, M., & Wakif, A. (2022). Numerical simulation of entropy transport in the oscillating fluid flow with transpiration and internal fluid heating by GGDQM. Waves in Random and Complex Media, 1-19.
[44] Chandrawat, R. K., Joshi, V., & Bég, O. A. (2022). Numerical study of time dependent flow of immiscible Saffman dusty (fluid-particle suspension) and Eringen micropolar fluids in a duct with a modified cubic B-spline Differential Quadrature method. International Communications in Heat and Mass Transfer, 130, 105758.
[45] Manjunatha, P. T., Gowda, R. P., Kumar, R. N., Suresha, S., & Sarwe, D. U. (2021). Numerical simulation of carbon nanotubes nanofluid flow over vertically moving disk with rotation. Partial Differential Equations in Applied Mathematics, 4, 100124.
[46] Prashu, P., Nandkeolyar, R., & Sangwan, V. (2022, March). Numerical simulation of non-uniform heat generation/absorption and dissipation effects on the unsteady MHD flow of a couple-stress dusty fluid. In AIP Conference Proceedings (Vol. 2435, No. 1). AIP Publishing.

[47] Bhatti, M. M., & Zeeshan, A. (2016). Analytic study of heat transfer with variable viscosity on solid particle motion in dusty Jeffery fluid. Modern Physics Letters B, 30(16), 1650196.

[48] Hayat, T., Rafiq, M., Alsaedi, A., & Ahmad, B. (2014). Radiative and Joule heating effects on peristaltic transport of dusty fluid in a channel with wall properties. The European Physical Journal Plus, 129, 1-17.

[49] Ramesh, K., & Devakar, M. (2017). Effect of heat transfer on the peristaltic transport of a MHD second grade fluid through a porous medium in an inclined asymmetric channel. Chinese Journal of physics, 55(3), 825-844.

[50] Nadeem, S., Akbar, N. S., Hayat, T., & Hendi, A. A. (2011). Peristaltic flow of Walter's B fluid in endoscope. Applied Mathematics and Mechanics, 32, 689-700.

[51] Hameed, M., Khan, A. A., Ellahi, R., & Raza, M. (2015). Study of magnetic and heat transfer on the peristaltic transport of a fractional second grade fluid in a vertical tube. Engineering Science and Technology, an International Journal, 18(3), 496-502.

[52] Muthuraj, R., Nirmala, K., & Srinivas, S. (2016). Influences of chemical reaction and wall properties on MHD peristaltic transport of a dusty fluid with heat and mass transfer. Alexandria Engineering Journal, 55(1), 597-611.

[53] Javed, M., & Hayat, T. (2017, January). Effects of heat transfer on MHD peristaltic transport of dusty fluid in a flexible channel. In 2017 14th international Bhurban conference on applied sciences and technology (IBCAST) (pp. 539-550). IEEE.

[54] Radhika, M., Punith Gowda, R. J., Naveenkumar, R., Siddabasappa, & Prasannakumara, B. C. (2021). Heat transfer in dusty fluid with suspended hybrid nanoparticles over a melting surface. Heat Transfer, 50(3), 2150-2167.

[55] Makinde, O. D., & Chinyoka, T. (2010). MHD transient flows and heat transfer of dusty fluid in a channel with variable physical properties and Navier slip condition. Computers & Mathematics with Applications, 60(3), 660-669.

[56] Singh, K., Rawat, S. K., & Kumar, M. (2016). Heat and mass transfer on squeezing unsteady MHD nanofluid flow between parallel plates with slip velocity effect. Journal of Nanoscience, 2016.

[57] Hafez, N. M., Alsemiry, R. D., Alharbi, S. A., & Abd-Alla, A. M. (2022). Peristaltic transport characteristics of a second-grade dusty fluid flown in a tube revisited: Role of heat transfer.

[58] Bhatti, M. M., Zeeshan, A., & Ijaz, N. (2016). Slip effects and endoscopy analysis on blood flow of particle-fluid suspension induced by peristaltic wave. Journal of Molecular Liquids, 218, 240-245.
[59] Tripathi, D., Jhorar, R., Bég, O. A., & Kadir, A. (2017). Electro-magneto-hydrodynamic peristaltic pumping of couple stress biofluids through a complex wavy micro-channel. Journal of Molecular Liquids, 236, 358-367.
[60] Bhatti, M. M., Zeeshan, A., Ellahi, R., & Shit, G. C. (2018). Mathematical modeling of heat and mass transfer effects on MHD peristaltic propulsion of two-phase flow through a Darcy-Brinkman-Forchheimer porous medium. Advanced Powder Technology, 29(5), 1189-1197.
[61] Ouaf, M. E., Abou-zeid, M., & Younis, Y. M. (2022). Entropy generation and chemical reaction effects on MHD non-Newtonian nanofluid flow in a sinusoidal channel. International Journal of Applied Electromagnetics and Mechanics, (Preprint), 1-21.
[62] Awais, M., Shah, Z., Perveen, N., Ali, A., Kumam, P., Rehman, H. U., & Thounthong, P. (2020). MHD effects on ciliary-induced peristaltic flow coatings with rheological hybrid nanofluid. Coatings, 10(2), 186.
[63] Kotnurkar, A. S., & Talawar, V. T. (2022). Impact of electro osmosis and joule heating effects on peristaltic transport with thermal radiation of hyperbolic tangent fluid through a porous media in an endoscope. Partial Differential Equations in Applied Mathematics, 5, 100340.
[64] Bhatti, M. M., Zeeshan, A., & Ellahi, R. (2016). Study of heat transfer with nonlinear thermal radiation on sinusoidal motion of magnetic solid particles in a dusty fluid. Journal of Theoretical and Applied Mechanics, 46(3), 75.
[65] Zeeshan, A., Ijaz, N., Bhatti, M. M., & Mann, A. B. (2017). Mathematical study of peristaltic propulsion of solid–liquid multiphase flow with a biorheological fluid as the base fluid in a duct. Chinese Journal of Physics, 55(4), 1596-1604.
[66] Hasona, W. M., El-Shekhipy, A., & Ibrahim, M. G. (2019). Semi-analytical solution to MHD peristaltic flow of a Jeffrey fluid in presence of Joule heat effect by using multi-step differential transform method. New Trends in Mathematical Sciences, 7(2), 123-137.
[67] Khan, A. A., Zafar, S., & Kanwal, A. (2021). Effect of relaxation and retardation times on dusty Jeffrey fluid in a curved channel with peristalsis. Advances in Mechanical Engineering, 13(6), 16878140211028454.
[68] Tariq, H., & Khan, A. A. (2020). Peristaltic flow of a dusty electrically conducting fluid through a porous medium in an endoscope. SN Applied Sciences, 2, 1-8.

[69] Ramesh, K., & Devakar, M. (2016). The effects of endoscope and heat transfer on the peristaltic flow of a second grade fluid in an inclined tube. Journal of Mechanics in Medicine and Biology, 16(04), 1650057.

[70] Das, S., Pal, T. K., & Jana, R. N. (2021). Electromagnetic hybrid Nano-blood pumping via peristalsis through an endoscope having blood clotting in presence of Hall and ion slip currents. Bio Nanoscience, 11(3), 848-870.

[71] Nadeem, S., Akhtar, S., Saleem, A., Akkurt, N., Almutairi, S., Ghazwani, H. A., & Eldin, S. M. (2023). Entropy analysis for a novel peristaltic flow in a curved heated endoscope: an application of applied sciences. *Scientific Reports*, *13*(1), 1504.

[72] Devakar, M., Ramesh, K., & Vajravelu, K. (2022). Magnetohydrodynamic effects on the peristaltic flow of couple stress fluid in an inclined tube with endoscope. Journal of Computational Mathematics and Data Science, 2, 100025.

[73] Das, S., Karmakar, P., & Ali, A. (2023). Simulation for bloodstream conveying bi-nanoparticles in an endoscopic canal with blood clot under intense electromagnetic force. Waves in Random and Complex Media, 1-38.